Published online 22 February 2017

Nucleic Acids Research, 2017, Vol. 45, No. 6 ***3323–3340***
doi: 10.1093/nar/gkx127

The *Schizosaccharomyces pombe* PPR protein Ppr10 associates with a novel protein Mpa1 and acts as a mitochondrial translational activator

Yirong Wang, Jianhua Yan, Qingzhen Zhang, Xuting Ma, Juan Zhang, Minghui Su, Xiaojun Wang and Ying Huang*

Jiangsu Key Laboratory for Microbes and Genomics, School of Life Sciences, Nanjing Normal University, 1 Wenyuan Road, Nanjing 210023, China

Received February 19, 2016; Revised February 07, 2017; Editorial Decision February 10, 2017; Accepted February 14, 2017

ABSTRACT

The pentatricopeptide repeat (PPR) proteins characterized by tandem repeats of a degenerate 35-amino-acid motif function in all aspects of organellar RNA metabolism, many of which are essential for organellar gene expression. In this study, we report the characterization of a fission yeast *Schizosaccharomyces pombe* PPR protein, Ppr10 and a novel Ppr10-associated protein, designated Mpa1. The *ppr10* deletion mutant exhibits growth defects in respiratory media, and is dramatically impaired for viability during the late-stationary phase. Deletion of *ppr10* affects the accumulation of specific mitochondrial mRNAs. Furthermore, deletion of *ppr10* severely impairs mitochondrial protein synthesis, suggesting that Ppr10 plays a general role in mitochondrial protein synthesis. Ppr10 interacts with Mpa1 *in vivo* and *in vitro* and the two proteins colocalize in the mitochondrial matrix. The *ppr10* and *mpa1* deletion mutants exhibit very similar phenotypes. One of Mpa1's functions is to maintain the normal protein level of Ppr10 protein by protecting it from degradation by the mitochondrial matrix protease Lon1. Our findings suggest that Ppr10 functions as a general mitochondrial translational activator, likely through interaction with mitochondrial mRNAs and mitochondrial translation initiation factor Mti2, and that Ppr10 requires Mpa1 association for stability and function.

INTRODUCTION

Mitochondria are eukaryotic organelles involved in many cellular functions including adenosine triphosphate (ATP) production through oxidative phosphorylation (OXPHOS), amino acid and fatty acid synthesis, apoptosis and the aging process in animals (1–4). The fission yeast *Schizosaccharomyces pombe* is an attractive model system for understanding mitochondrial gene expression (5). Like the animal mitochondrial genomes (mtDNA), the mtDNA of *S. pombe* is a compact, circular DNA of ∼19 kb. It primarily encodes apocytochrome *b* (Cob1, also called Cob or Cytb) of ubiquinol-cytochrome *c* reductase (cytochrome *b-c1* complex or complex III), cytochrome *c* oxidase (COX or complex IV) subunits 1, 2, 3 (Cox1, Cox2 and Cox3), ATP synthase (complex V) subunits 6, 8, 9 (Atp6, Atp8 and Atp9), a mitochondrial ribosomal protein (Var1, also called Rps3), 2 rRNAs (*rnl* and *rns*), 25 tRNAs and the RNA subunit of RNase P (*rnpB*).

Pentatricopeptide repeat (PPR) proteins play essential roles in both transcriptional and post-transcriptional control of mtDNA-encoded gene expression (6–9), including RNA 5′-end maturation, intron splicing, RNA editing in plant organelles, RNA stabilization and translational activation. PPR proteins are found in the organelles of nearly all eukaryotes but absent from almost all bacteria. These proteins are most abundant in higher plants, with probably up to 450 proteins in *Arabidopsis thaliana* (10). In contrast, fungi and metazoans have a small number of PPR proteins. The budding yeast *Saccharomyces cerevisiae*, *S. pombe* and humans have only 15, 10 and 7 PPR proteins, respectively (7,8). The extraordinarily large number of PPR proteins in higher plants reflects that the post-transcriptional processes in plant organelles are much more complex.

Typical PPR proteins are characterized by 2–30 tandem repeats of a degenerate ∼35-amino-acid (aa) repeat. PPR motifs are mainly involved in sequence-specific RNA-binding. For example, PPR motifs in *S. cerevisiae* Pet309 were shown to act cooperatively to promote a high affinity interaction with the *COX1* mRNA (11). The RNA binding specificity of PPR proteins is primarily determined by amino acids at positions 4 and 34 within the repeats (12–15). Structural studies reveal that each PPR repeat folds into a

*To whom correspondence should be addressed. Tel: +86 25 85891263; Fax: +86 25 85891263; Email: y_shang_hai@126.com; yhuang@njnu.edu.cn

pair of anti-parallel α-helices connected by a loop (16–20) and can interact with a single nucleotide (17).

Mitochondrial translation appears to be controlled by different mechanisms in yeast and mammalians. Both *S. cerevisiae* and *S. pombe* mtDNA-encoded mRNAs (mt-mRNAs) contain 5′-untranslated regions (5′-UTRs) that can be targeted for translational control. Indeed, the *S. cerevisiae* mitochondrial translational activators can bind to the 5′-UTRs of their respective cognate mRNAs (21–23). In *S. cerevisiae*, translation of *COX1*, *COX2*, *COX3* and *CYTB* mRNAs requires specific nuclear-encoded proteins: Pet309/Mss51/Mam33 for *COX1* (21,24–26), Pet111 for *COX2* (23,27), Pet54/Pet122/Pet494 for *COX3* (28–31) and Cbp3/Cbp6 for *CYTB* (32). Mss51 and Cpb6/Cpb3 also promote assembly of Cox1 and Cytb, respectively, into their respective complexes (32,33). Among the *S. cerevisiae* mitochondrial translational activators, only Pet309 and Pet111 are PPR proteins. Except for homologs of Mss51, Mam33, Cpb3 and Cpb6, no other sequence homologs of *S. cerevisiae* mitochondrial translational activators can be found in *S. pombe*. Similarly, no human homologs of the *S. cerevisiae* translational activators can be found by BLAST analysis.

Mammalian mt-mRNAs do not have 5′-UTRs. Thus, different mechanisms may be used to regulate mRNAs translation in mammalian mitochondria. Two mammalian mitochondrial translational activators have been identified so far. LRPPRC (leucine-rich pentatricopeptide repeat-containing) is a PPR protein required for the stabilization and translation of both *COX1* and *COX3* mRNAs and thus, LRPPRC is considered to be a possible mammalian functional homolog of yeast Pet309 (34,35). However, LRPPRC is a multifunctional protein that controls mRNA stability, mRNA polyadenylation and translation in human mitochondria (36–38). Mutations in human *LRPPRC* cause the French-Canadian-type Leigh syndrome, a neurodegenerative disorder caused by deficiency in COX (34). TACO1, a non-PPR protein, is specifically required for translation of *COX1* mRNA in mice and humans, but the mechanism is unknown (39,40). Interestingly, the sequence homologs of TACO1 exist in both *S. cerevisiae* and *S. pombe*.

A genome-wide analysis of PPR proteins in *S. pombe* reveals that *S. pombe* Ppr1-9 (In *S. pombe*, PPR proteins are numbered sequentially from 1) modulate mitochondrial RNA expression (41). These PPR proteins contain 2–18 PPR motifs and do not show significant homology to other PPR proteins outside the PPR motifs. Ppr9 (Rpo41) is the mitochondrial core RNA polymerase. Ppr1 is required for the stability of both the *cox2* and *cox3* mRNAs. Ppr3, Ppr6 and Ppr7 are required for accumulation of 15S rRNA, *atp9* mRNA and *atp6* mRNA, respectively. While Ppr2 is a general mitochondrial translation factor, Ppr4 is a translational activator specific for Cox1. Ppr8 appears to have a limited role in mitochondrial translation. Ppr5 seems to be a general negative regulator of mitochondrial translation. However, the molecular mechanism of action of these PPR proteins is still unclear.

Here, we present functional characterization of a newly identified PPR protein from *S. pombe*, Ppr10 and its associated protein Mpa1. We demonstrate that both Ppr10 and Mpa1 play a role in synthesis of mtDNA-encoded proteins and that impaired mitochondrial protein synthesis caused by *ppr10* or *mpa1* deletion results in respiratory defects. We also show that Mpa1 is required for the normal function of Ppr10.

MATERIALS AND METHODS

Yeast strains, media and genetic manipulation and PCR primers

The *S. pombe* strains used in this study are listed in Supplementary Table S1. *ppr10*, *mpa1* and *lon1* were deleted by the one-step gene replacement method (42). Briefly, the 5′ flank (393 bp) and 3′ flank (505 bp) of *ppr10*, the 5′ flank (799 bp) and 3′ flank (864 bp) of *mpa1* and the 5′ flank (1041 bp) and 3′ flank (828 bp) of *lon1* were amplified by PCR. The PCR products for the 5′ and 3′ flanks of *ppr10* were cloned into the SalI/BglII and SacI/EcoRI sites of pFA6a-kanMX6 (43), respectively, generating the Δ*ppr10::kanMX6* deletion cassette construct. The PCR products for the 5′ and 3′ flanks of *mpa1* were cloned into the SmaI/BglII sites and SacI/SpeI sites of pFA6a-kanMX6, respectively, generating the Δ*mpa1::kanMX6* deletion cassette construct. The PCR products for the 5′ and 3′ flanks of *lon1* were cloned into the SmaI/BglII sites and SacI/SpeI sites of pFA6a-hphMX6, respectively, generating the Δ*lon1::hphMX6* deletion cassette construct. The Δ*ppr10::kanMX6* deletion cassette and Δ*mpa1::kanMX6* deletion cassette were transformed into the wild-type (WT) strain yHL6381, generating yHH1 and yZQ1, respectively. The Δ*lon1::hphMX6* deletion cassette was transformed into yYJ5, the yHL6381-derived strain that contains 13Myc-tagged Ppr10, generating ySM1. The Δ*lon1::hphMX6* deletion cassette was also transformed into single deletion mutants yYJ6 and yHH1 to generate double deletion mutants ySM2 and ySM3, respectively. All deletions were verified by PCR and loss of expression of deleted genes was verified by qRT-PCR.

Strains carrying the epitope-tagged genes were created by homologous recombination at the C-termini of the genes. Plasmid pTAPkan1 (44) was used for the introduction of the tandem affinity purification (TAP) tag into *ppr10*. pFA6a-13Myc-kanMX6 (43) with the *kanMX6* marker or pFA6a-13Myc-ura4 with the *ura4* marker were used for the introduction of a 13Myc tag into *ppr10*. Plasmid pFA6a-3HA-leu1 was used for the introduction of the 3HA tag into *mpa1*. Plasmid pFA6a-2FLAG-ura4 was used for the introduction of the 2FLAG tag into Tom20 (SPAC6F12.07), Mti2 (SPBC1271.15c) and Mti3 (SPBC23G7.03). All epitope tags were added at the C-termini and all epitope-tagged strains were verified by PCR, DNA sequencing and western blot analysis. To integrate *mpa1* into the chromosomal *leu1-32* site, integrating plasmid pJK148-1500-mpa1-3HA encoding 3HA-tagged *mpa1* under the control of its endogenous promoter was linearized with NruI and transformed into strain yYJ8.

S. pombe cells were grown in yeast extract medium (YES, 0.5% yeast extract medium) or yeast nitrogen base minimal selective medium (YNB, 0.67% yeast nitrogen base without amino acids, 2% glucose and supplements) with appropriate supplements (45). These media were also supplemented with either 3% glucose, 6% glycerol or 4% galactose and

0.1% glucose as indicated. For growth assays on solid media, 10-fold serial dilutions of cells were spotted onto agar plates and grown at 30°C.

Standard media and protocols for genetic manipulation of fission yeast were used as described previously (45). Primer sequences used for PCR cloning, gene deletion and epitope tagging are available upon request.

Construction of plasmids

Plasmid pFA6a-3HA-leu1 with the *leu1* marker was constructed by replacing a 1.4-kb BglII-SacI fragment containing kanMX6 of plasmid pFA6a-3HA-KanMX6 (43) with 2.1-kb of the *leu1* marker from pJK148 (46). Plasmid pFA6a-13Myc-ura4 was constructed by replacing the kanMX6 marker from plasmid pFA6a-13Myc-kanMX6 (43) with 1.8-kb of the *ura4* marker from plasmid pREP4X (47). pFA6a-2FLAG-ura4 is derived from pFA6a-3HA-kanMX6 (43) first by replacing the kanMX6 fragment with the *ura4* marker from pREP4X and then by replacing the 3HA tag with the 2FLAG tag. For the latter, a pair of complementary oligonucleotides (sense, 5′-CCGGGGACTACAAGGACGACGATGAC AAGGATTACAAAGATGACGACGA; antisense, 5′-CGCGGCCTCACTTATCGTCGTCATCTTTGTAATC CTTGTCATCGTCGTCCTTGTAGTCC) were annealed and ligated into pFA6a-3HA-ura4 digested with SmaI and BssHII. To construct plasmid pJK148-1500-mpa1-3HA, a DNA fragment containing 1.5-kb of upstream, 3HA-tagged *mpa1* coding sequence and *adh1* terminator sequence were amplified from the genomic DNA isolated from strain yYJ2. The PCR product was digested with SpeI and EcoRI and ligated into the SpeI/EcoRI-digested integrating plasmid pJK148.

Plasmid pFA6a-hphMX6 was constructed by replacing with kanMX6 with the hygromycin B resistance cassette (hphMX6) containing the *Escherichia coli* hygromycin B resistance gene (*hph*) under the control of the *Ashbyu gossypii TEF* promoter, a strong, constitutive promoter of the translation elongation factor gene. The hphMX6 marker was made by overlap PCR to join together three overlapping PCR fragments containing 383-bp of the *TEF* promoter, 1.0-kb of the *hph* coding sequence and 236-bp of the *TEF* terminator. The promoter and terminator sequences of *TEF* and the *hph* coding sequence are amplified from pFA6a-kanMX6 (43) and pAN7-1 (48), respectively. The PCR product was digested with BglII and SacI and ligated into the BglII/SacI sites of pFA6a-kanMX6.

S. pombe expression vectors were constructed as follows. The coding region of *ppr10* was PCR-amplified from *S. pombe* genomic DNA. The PCR product was digested with XhoI/SmaI and cloned into the XhoI/SmaI sites of the *S. pombe* expression vector pREP82X containing the thiamine-repressible *nmt1* promoter (47), generating pREP82X-ppr10. Plasmid for expressing *ppr10* lacking the two predicted PPR motifs was prepared by overlap PCR using pREP82X-ppr10 as template and two pairs of PCR primers including a pair of overlapping primers containing the deleted region. The PCR product was cloned into the XhoI/SmaI sites of pREP82X, generating pREP82X-ppr10ΔPPR. Plasmid for expressing 5FLAG-tagged *ppr10* was constructed by cloning the coding region of *ppr10* into the XhoI/BamHI sites of plasmid pREP82X-5FLAG, generating pREP82X-5FLAG-ppr10. pREP82X-5FLAG was constructed by inserting a 5FLAG tag into the SmaI site of pREP82X. Plasmid for expressing 5FLAG-tagged *ppr10* lacking the PPR motifs was prepared by PCR using the plasmid pREP82X-ppr10ΔPPR as template. The PCR product was cloned into the XhoI/BamHI sites of pREP82X-5FLAG, generating pREP82X-5FLAG-ppr10ΔPPR.

Plasmids for glutathione S-transferase (GST) pull-down experiments were constructed as follows: the coding sequences of *ppr10*, *mpa1*, *mti2* and *mti3* were amplified by PCR from genomic DNA, and cloned into the BamHI/SmaI sites of pGEX-4T-1 for *ppr10*, the NdeI/XhoI sites of pET30a for *mpa1*, the EcoRI/SalI sites of pET28a for *mti2* and the NcoI/XhoI sites of pET28a for *mti3*, generating plasmid pGEX-4T-1-ppr10-N-GST, pET30a-mpa1-C-His, pET28a-mti2 and pET28a-mti3, respectively.

Measurement of mtDNA copy number

Yeast cells were grown in 10 ml of YES medium at 30°C to mid-log phase. Genomic DNA was isolated from spheroplasts as described (49). DNA was quantified using the NanoDrop 2000 spectrophotomer (Thermo Scientific). MtDNA copy number was determined by quantitative real-time PCR (qPCR) using primer pairs (for primer sequences, see Supplementary Table S2) as previously defined (49). Various dilutions of the template DNA were used to ensure measurements were within the linear range. The median of the C_T values for mtDNA-encoded genes (*cob1*, *cox1*, *cox3* and *atp9*) and the median of the C_T values for nuclear genes (*spo12*, *ace2* and *exg1*) were used to estimate mtDNA and nuclear DNA levels, respectively. The ΔC_T value was calculated by subtracting the median C_T value for mtDNA from the median C_T value for nuclear DNA. The fold change in the mtDNA copy number of each mutant strain compared to that of WT strain (whose value was set to 1) was calculated using the equation $2^{-\Delta\Delta Ct}$ (the $\Delta\Delta C_T$ method).

Quantitative real-time RT-PCR

WT and Δ*ppr10* cells were grown overnight in YES medium. The cultures were then diluted to an OD_{600} of 0.2 in the same medium. Diluted cultures were grown until OD_{600} reached 0.6–0.8, and cells were harvested. RNA was isolated using an E.Z.N.A.® Yeast RNA Kit (OMEGA). Isolated RNA was treated with RNase-free DNase I (Fermentas) to remove contaminating genomic DNA. RNAs were reverse-transcribed using the iScript cDNA Synthesis Kit (Bio-Rad). Quantitative Real-Time RT-PCR (qRT-PCR) was performed using SYBR Select Master Mix (Life Technologies) with each primer sets (Supplementary Table S2). All reactions were performed in triplicate. Data analysis was performed by StepOne™ software. The threshold cycle number (C_T) values were normalized by subtracting the mean C_T value of histone H2B (*htb1*) mRNA. The relative levels of expression of mitochondrial-encoded RNAs (mt-RNAs) were calculated by using the $2^{-\Delta\Delta Ct}$ method.

Northern blot analysis

Total RNA was isolated from *S. pombe* cells grown exponentially in rich YES medium using the hot phenol method as described (50). The RNA was separated on a 1% agarose-6.8% formaldehyde gel or a 6% polyacrylamide-7 M urea gel and blotted onto a Biodyne B Nylon Membrane (Thermo Scientific). Northern blot analysis was carried out as described previously (51). For detection of mature mt-tRNAs, *atp9*, *rnpB* and *var1* RNAs, oligonucleotides were used as probes. Sequences for oligonucleotide probes are shown in Supplementary Table S2. For detection of other mtDNA-encoded RNAs, probes were obtained by PCR amplification of *S. pombe* mtDNA with pairs of specific oligonucleotide primers (Supplementary Table S2). All probes were 5′-end-labeled by [γ-^{32}P]ATP (BLU002Z; Perkin-Elmer Life Science) and T4 polynucleotide kinase according to the manufacturer's instructions. Signals were detected by using the Cyclone Plus Storage Phosphor System (Perkin-Elmer).

RNA immunoprecipitation

RNA immunoprecipitation (RIP) was performed as described (11). WT cells expressing chromosomally encoded TAP-tagged Ppr10 (yWP1) or untagged Ppr10 (yHL6381) were grown in YES medium and harvested after reaching an OD_{600} of 2.0. Mitochondria were isolated as described below. A total of 200 μg of mitochondria were lysed in 200 μl of lysis buffer [20 mM Tris-HCl pH 7.4, 100 mM NaCl, 0.7% n-Dodecyl β-D-maltoside (DDM), 200 U of RNaseOUT (Invitrogen) and protease inhibitors. Insoluble material was removed by centrifugation at 12 000 $\times g$ for 10 min at 4°C. The mitochondrial extracts were diluted 1:2 with lysis buffer without DDM and incubated with 20 μl of IgG agarose beads for 4 h at 4°C under constant rotation. After extensive washing with lysis buffer, bound RNAs were eluted by incubating the beads in tobacco etch virus protease cleavage buffer (10 mM Tris-HCl pH 8.0, 300 mM NaCl, 0.1% Igepal CA-630, 200 U/ml RNaseOUT, 170 U/ml tobacco etch virus and protease inhibitors) for 3 h at 16°C. Both total RNA and immunoprecipitated RNA were extracted by using phenol and purified by using the miRNeasy Micro Kit (Qiagen). Purified RNAs were reverse-transcribed with the iScript cDNA Synthesis Kit (Bio-Rad). The cDNA was used as the template to using 2XPCR Taq Master Mix (ABM) and primers (Supplementary Table S2) that amplify the 5′-UTRs of mtDNA-encoded genes. It should be noted that RT-PCR is not quantitative under the conditions used here. The resulting PCR products were detected on 1.5% agarose gel.

Purification of mitochondria, subfractionation of mitochondria and protease treatment of mitochondria

Mitochondria were isolated from *S. pombe* spheroplasts prepared using lysing enzymes from *Trichoderma harzianum* (Sigma), and crude mitochondrial extracts were prepared essentially as described (52). Further purification of mitochondria was done according to the reference (53). Briefly, crude mitochondrial fractions were loaded onto a 15–60% (w/v) sucrose gradient, ultracentrifuged at 33 000 rpm for 1 h at 4°C in a Beckman SW55Ti rotor. The mitochondria were then collected, suspended in the Sucrose-EDTA-MOPS (SEM) buffer (250 mM sucrose, 1 mM ethylenediaminetetraacetic acid, 10 mM MOPS, pH 7.2), and centrifuged for 15 min at 12 000 rpm. The mitochondrial pellets were washed with the SEM buffer and resuspended in the SEM buffer to a protein concentration of ∼5 mg/ml. For protease treatment, mitochondrial preparation was treated with or without 50 μg/ml proteinase K in the presence or absence of 0.2% Triton X-100 for 30 min and digestion was stopped with 1 mM phenylmethylsulfonylfluoride (PMSF) (54). Proteins were precipitated with 30% trichloroacetic acid, washed with chilled acetone, resuspended in sodium dodecyl sulphate-polyacrylamide gel electrophoresis (SDS-PAGE) loading buffer and subjected to SDS-PAGE and western blotting. Isolation of membrane and soluble mitochondrial proteins from mitochondria was performed by sodium carbonate treatment (55).

Pulse-labeling of mitochondrial translation products

In vivo labeling of mitochondrial translation products was performed according to (56) except that anisomycin was used as an inhibitor of cytosolic translation. Basically, WT, Δ*ppr10* and Δ*mpa1* cells were cultured to exponential phase in complete medium containing 0.1% glucose and 5% raffinose. A total of 1.5 OD_{600} of yeast cells were collected and suspended in 500 μl of reaction buffer containing 1 mg/ml anisomycin. After 15 min preincubation at 30°C, 8 μl of [^{35}S]-methionine/cysteine mix (NEG-072; Perkin-Elmer Life Science) was added and the cell suspensions were incubated at 30°C for 1.5 h. After labeling, cells were pelleted by centrifugation at 10 000 *g* for 1 min. The cell pellet was then suspended in 75 μl solubilization buffer [1.8 M NaOH, 1 M β-mercaptoethanol, 10 mM PMSF] and 500 μl of H_2O was added to dilute the cell solubilization buffer. Proteins were precipitated by addition of an equal volume of 50% trichloroacetic acid. The precipitates were washed, solubilized in SDS-PAGE loading buffer, and then separated by SDS-PAGE electrophoresis. The proteins were blotted onto nitrocellulose membranes and signals were detected by using the Cyclone Plus Storage Phosphor System (Perkin-Elmer).

Affinity purification, co-immunoprecipitation (co-IP) and GST pull-down assay

Cells expressing chromosomally encoded Ppr10-TAP were grown in 1 l YES medium to an OD_{600} of 2.0 and harvested. Cell pellets were washed and resuspended in 4 ml lysis buffer (6 mM Na_2HPO_4, 300 mM NaCl, 4 mM NaH_2PO_4, 1% Igepal CA-630, 50 mM NaF, 4 μg/ml leupeptin, 4 μg/ml pepstatin A, 0.1 mM Na_3VO_4 and 1 mM PMSF) and broken in a bead beater (FastPrep-24; MP Biomedical). Lysates were clarified by centrifugation for 30 min at 12 000 *g*. Ppr10-TAP was sequentially affinity-purified using rabbit IgG agarose beads (Sigma-Aldrich) and calmodulin affinity resin (Agilent Technologies) columns according to the reference (57). Copurifying proteins were identified using the UltrafleXtreme™ MALDI-TOF/TOF mass spectrometer (Bruker Daltonics).

For co-IP between endogenous Ppr10 and Mpa1, whole cell extracts were prepared from cells expressing chromosomally encoded Mpa1-HA (yWP2, negative control) or Ppr10-Myc and Mpa1-HA (yYJ3). Proteins were precipitated using EZview™ Red anti-*c*-Myc affinity gel (Sigma-Aldrich). The beads were washed five times in 20 mM Tris-HCl pH 8.0, 137 mM NaCl, 1% Igepal CA-630. The bound proteins were eluted by 55°C for 10 min in loading buffer and detected by western blotting with anti-*c*-Myc and anti-Mpa1 antibodies (Abs). Reciprocal co-IP was performed using extracts prepared from cells expressing Ppr10-Myc or Ppr10-Myc and Mpa1-HA. Proteins were precipitated with EZview™ Red anti-HA affinity gel (Sigma-Aldrich) and were detected by western blotting using anti-Mpa1 and anti-*c*-Myc Abs. Extracts were also treated with 0.05 mg/ml RNase A for 30 min at 25°C prior to immunoprecipitation (IP). To evaluate the effect of RNase A treatment, total RNA was isolated using an E.Z.N.A.® Yeast RNA Kit, and RNA concentration was determined using the Nanodrop 2000 spectrophometer. The total RNA concentration was reduced by 20-fold after RNase A treatment.

For co-IP between Ppr10 and Mti2 or Mit3, protein extracts were prepared from cells expressing chromosomally encoded Ppr10-Myc and Mti2-FLAG (yYJ11) or Ppr10-Myc and Mti3-FLAG (yYJ13), respectively. The beads were washed once in 20 mM Tris-HCl pH 8.0, 137 mM NaCl, 1% Igepal CA-630, twice in 10 mM Tris-HCl pH 8.0, 68.5 mM NaCl, 0.5% Igepal CA-630 and twice in 5 mM Tris-HCl pH 8.0, 34.3 mM NaCl, 0.25% Igepal CA-630. Western blotting using anti-*c*-Myc and anti-FLAG Abs.

For GST pull-down, *E. coli* cells co-expressing Ppr10-GST and Mpa1-His or GST and Mpa1-His were suspended in phosphate buffered saline containing 1 mM PMSF and lysed by sonication. The cell lysates were incubated with glutathione Sefinose™ resin (Sangon Biotech) overnight at 4°C. Beads were extensively washed with phosphate buffered saline, and eluted with 10 mM GSH. The bound materials were resolved by SDS-PAGE and subjected to western blotting using anti-GST and anti-His Abs.

Production of Abs

Polycolonal antisera were raised in rabbits against synthetic peptides corresponding to amino acids (aa) 524–537 of Cox1, aa 149–162 of Cox2, aa 123–136 of Cox3, aa 256–268 of Cob1, aa 2–21 of Atp6 and aa of 300–319 of Mpa1. To generate anti-Cox4 Ab that recognizes the *S. pombe* COX subunit 4 and anti-Trz2 Ab that recognizes the *S. pombe* mt-tRNA 3′-end processing enzyme, full-length open reading frames of *cox4* and *trz2* were PCR amplified from the genomic DNA. The resulting PCR products were cloned into the NcoI/XhoI sites of pET30a and NdeI/XhoI sites of pET28a, respectively. Recombinant 6His-tagged proteins were expressed in *E. coli* strain BL21 (DE3), purified by Ni-NTA agarose chromatography (Qiagen) and used for antiserum production.

Western blot analysis

S. pombe whole cell extracts were prepared by alkaline extraction (58) or by breaking cells with glass beads using a FastPre-24 bead beater (MP Biomedicals) (59). Mitochondrial protein extracts were prepared as described above. Proteins were resolved by electrophoresis on SDS-PAGE, and the separated protein bands were transferred electrophoretically to a Hybond ECL transfer membrane (GE healthcare). Blots were probed with anti-Cox1 (1:1000), anti-Cox2 (1:1000), anti-Cox3 (1:400), anti-Cox4 (1:1000) and anti-Cob1 (1:500), anti-Trz2 (1:1000), anti-Sla1 (1:5000), anti-HSP60 (1:1000; Sangon Biotech), anti-FLAG (1:000; Sigma), anti-CBP (1:1000; GenScript), anti-HA (1:2000; Sigma-Aldrich), anti-*c*-Myc (1:2000; Affinity Biotech), anti-His (1:2000; GenScript) and anti-GST (1:2000; GenScript) Abs. Secondary Abs used were IRDye 800CW conjugated goat anti-rabbit or anti-mouse Abs (LI-COR Biosciences). Bands were detected using an Odyssey near-infrared fluorescence scanner (LI-COR Biosciences).

RESULTS

Ppr10 is a *Schizosaccharomyces* specific protein

Ppr10 (Systematic name: SPBC106.19) has been recently identified as a candidate *S. pombe* PPR protein using the SCIPHER algorithm and profiles constructed from multiple sequence alignment of PPR proteins from available yeast genomes including the genomes from three additional *Schizosaccharomyces* species (7). Recent work by Bonnefoy *et al*. has suggested that Ppr10 plays a general role in mt-RNA expression; however, the data have not been published (7). This protein has a molecular size of 59 kDa (515 amino acids) and is classified as orphan in the *S. pombe* genome database, PomBase (http://www.pombase.org/). A standard BLAST search, with Ppr10 as the query, revealed that close homologs of Ppr10 exist only in other recently sequenced fission yeast species, *Schizosaccharomyces octosporus* (Systematic name: EPX73444.1), *Schizosaccharomyces cryophilus* (Systematic name: EPY51084.1) and *Schizosaccharomyces japonicas* (Systematic name: EEB09734.2).

Protein sequence analysis using the PPR repeat prediction program TPRpred (http://toolkit.tuebingen.mpg.de/tprpred) revealed that *S. pombe* Ppr10 and all of its homologs contain putative PPR motifs. *S. pombe* Ppr10 contains 2 degenerate PPR motifs (^{253}TAIDRSLLALLSTG ELEAALELLVYLKNNNIPIND^{287} and ^{288}AYLRMMVI NFCLANKPTLAVRFCQAWFKQSKMLSS^{322}) (Supplementary Figure S1), which are located near the center of the protein. Ppr10 proteins from *S. octosporus*, *S. cryophilus* and *S. japonicas* contains 7, 4 and 6 putative PPR motifs, respectively (data not shown). Besides the predicted PPR motifs, no other conserved motifs could be identified in fission yeast Ppr10 proteins.

Protein secondary structure prediction using PSIPRED software (http://bioinf.cs.ucl.ac.uk/psipred/) revealed that *S. pombe* Ppr10 is composed entirely of α-helices and connecting loops, suggesting that the protein may contain a large number of PPR motifs (Supplementary Figure S2).

The Δ*ppr10* mutant exhibits a range of phenotypes reflecting impaired respiration

To investigate the biological function of *ppr10*, we tested whether deletion of *ppr10* affected cell growth on different media. Like other respiration-deficient mutants (41,60,61), the Δ*ppr10* mutant grew very slowly on glycerol- and galactose-containing rich media, which allow only respiratory growth (Figure 1A). Thus, the inability of cells to grow on glycerol- and galactose-containing media implies defects in mitochondrial respiration. The Δ*ppr10* mutant exhibited a mild slow-growth phenotype when grown on glucose-containing rich medium (YES) where respiration also occurs but to a lesser extent. We examined the sensitivity of the Δ*ppr10* mutant to the electron transport chain complex III inhibitor antimycin A. Antimycin A has been shown to severely inhibit cell growth only when the glucose concentration in the media is lowered to 0.08% (62). As expected, the WT strain was insensitive to antimycin A when grown on YES medium containing 3% glucose (Figure 1B). It has also been shown that *in S. pombe* some respiratory mutants are hypersensitive to antimycin A on YES plates, likely because a basal level of mitochondrial respiratory activity is required for the viability of *S. pombe* cells even when cells are grown under fermentation conditions (41,60). The Δ*ppr10* mutant was unable to grow on YES medium containing 100 μg/ml antimycin A (Figure 1B). As controls, we also examined the sensitivity of the Δ*ppr2* (*ppr2* is a general mitochondrial translation factor) and Δ*ppr6* (*ppr6* is required for *atp9* mRNA stability) mutants to antimycin A. Consistent with the previous findings (41), the Δ*ppr6* mutant could not grow on plates containing antimycin A, whereas the growth of the Δ*ppr2* mutant was modestly affected. Altogether, these results indicate that the Δ*ppr10* mutant is defective in mitochondrial respiration.

To determine if the two predicted PPR motifs are important for the function of Ppr10, we constructed plasmids expressing either WT or mutated PPR protein lacking the predicted PPR motifs under the control of pREP82X-nmt1 promoter (47). These plasmids, along with the empty vector pREP82X, were used to transform individually into the Δ*ppr10* mutant. As a control, pREP82X was also used to transform into the WT strain. We used YNB medium instead of EMM medium for selective cultivation of plasmid-containing cells for the reason that Δ*ppr10* cells grow extremely slowly in EMM medium. We examined the growth of these strains on YNB media containing either glucose, glycerol or galactose as the carbon source. The WT Ppr10, but not the empty vector and the mutant Ppr10 lacking the predicted PPR motifs, could rescue the growth defects caused by deletion of *ppr10* (Figure 1C). Both the WT and mutant Ppr10 proteins were expressed at similar levels as judged by western blotting of extracts prepared from the Δ*ppr10* mutant expressing 5FLAG-tagged WT and mutant Ppr10 (Figure 1D). These results indicate that the PPR motifs are essential for the biological function of Ppr10.

We also examined the viability of WT and the Δ*ppr10* mutant cells at different stages of the growth by spotting cultures onto rich glucose medium plates or by plating cells onto rich glucose medium to count the total number of viable colonies. The Δ*ppr10* mutant lost viability much more rapidly than the WT strain (Figure 1E and F). At 72 h, the viability of Δ*ppr10* cells dropped below 1% whereas the viability of WT cells dropped to ∼55%. These results are consistent with the previous findings that *S. pombe* respiratory-deficient mutants have a reduced viability at stationary phase (63).

Δ*ppr10* cells exhibited morphological changes. Most Δ*ppr10* cells were stubby while a few looked round, branched or elongated (Supplementary Figure S3A). In addition, microscopic examination also revealed that Δ*ppr10* cells were attached to each other. Indeed, Δ*ppr10* cells exhibited non-sexual flocculation when grown in YES medium (Supplementary Figure S3B). The flocculation of Δ*ppr10* cells was prevented by addition of galactose or raffinose (data not shown).

The level of mtDNA is mildly reduced in Δ*ppr10* cells

To analyze mtDNA copy number in Δ*ppr10* cells, we performed real-time qPCR for mtDNA-encoded genes (*cob1*, *cox1*, *cox3* and *atp9*) and nuclear DNA-encoded genes (*spo12*, *ace2* and *exg1*) on genomic DNA derived from WT and Δ*ppr10* cells. A *ptp1-1* mutant strain (Cy0989) depleted of mtDNA (49,64) was included as a negative control. This mutant strain contains a nuclear mutation, *ptp1-1*, which allows *S. pombe* cells to grow in the absence of mtDNA (49,64). The median of C_T values from four mtDNA-specific primers and the median of C_T values from three nuclear DNA-specific primers were used to estimate the relative copy number of mtDNA. As shown in Figure 2A, the mtDNA copy number in Δ*ppr10* cells was reduced to ∼83% of that in the WT strain. As a control, mtDNA copy number in the *ptp1-1* mutant dropped to nearly zero. These results indicate that deletion of *ppr10* causes a mild loss of mtDNA copy number, but does not lead to depletion of mtDNA.

Ppr10 is required for the accumulation of *cox1*, *cob1*, *atp8* and *atp9* mRNAs

To investigate whether *ppr10* deletion could affect accumulation of mt-mRNAs, *rnpB* and mt-rRNAs, we isolated total RNA from the Δ*ppr10* mutant and its isogenic WT strain, and performed qRT-PCR using gene-specific primer pairs. We found that the level of *cox1* mRNA was dramatically reduced to a barely detectable level in Δ*ppr10* cells (Figure 2B). In addition, the levels of *cob1*, *atp8* and *atp9* mRNAs were reduced in Δ*ppr10* cells. The abundance of other mt-RNAs analyzed here was not significantly changed (Figure 2B). Furthermore, northern blotting confirmed that *cox1* and, to a lesser degree, *cob1*, *atp8* and *atp9* mRNAs were dramatically reduced in Δ*ppr10* cells, whereas the levels of other mt-RNAs analyzed were not apparently changed (Figure 2C).

To address the possibility that *ppr10* deletion affected tRNA accumulation, we isolated total RNA from the Δ*ppr10* mutant and its isogenic WT strain and performed northern blot analysis of tRNA. We chose to analyze seven mt-tRNAs, some of which have previously been shown to have dramatically reduced levels of mature forms when processing of their 3′-ends was affected in the mutant deficient

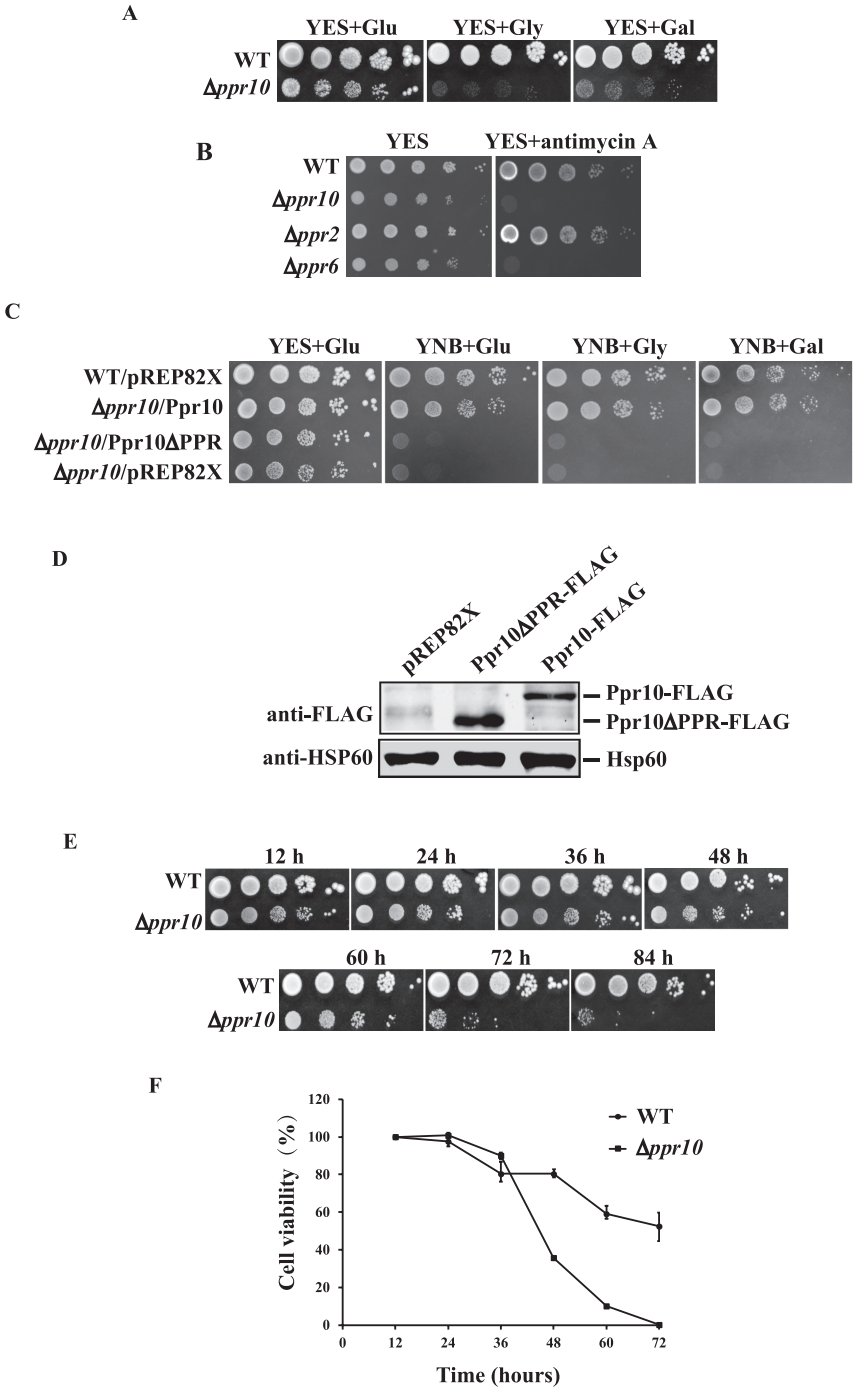

Figure 1. Δ*ppr10* cells exhibit a range of phenotypes indicative of defective mitochondrial respiration. (**A**) Growth defects of Δ*ppr10* cells on various media. WT and Δ*ppr10* cells were grown in YES medium to stationary phase and 10-fold serial dilutions were spotted onto rich media containing 3% glucose (YES+Glu), 6% glycerol (YES+Gly) or 4% galactose and 0.1% glucose (YES+Gal). Plates were incubated at 30°C for 6–7 days. (**B**) Δ*ppr10* cells are highly sensitive to antimycin A. Stationary-phase WT, Δ*ppr10*, Δ*ppr2* and Δ*ppr6* cells were spotted in 10-fold serial dilution onto YES plates in the absence or presence of 100 μg/ml antimycin A and grown at 30°C for 2–3 days. (**C**) The PPR motifs of *S. pombe* Ppr10 are required for respiratory growth. A 10-fold dilution series of WT cells carrying empty plasmid pREP82X (WT/pREP82X), or Δ*ppr10* cells carrying pREP82X-Ppr10 expressing full-length Ppr10 (Δ*ppr10*/Ppr10), pREP82X-Ppr10ΔPPR expressing Ppr10 lacking two predicted PPR motifs (Δ*ppr10*/Ppr10ΔPPR) or pREP82X (Δ*ppr10*/pREP82X) was spotted onto YES or YNB plates containing 3% glucose (YNB+Glu), 6% glycerol (YNB+Gly) or 4% galactose and 0.1% glucose (YNB + Gal), and grown at 30°C. (**D**) A western blot shows the expression of full-length Ppr10 and a mutant lacking the PPR motifs. Extracts were prepared from Δ*ppr10* cells carrying pREP82X, or a plasmid either expressing 5FLAG-tagged full-length Ppr10 (Ppr10-FLAG) or mutant Ppr10 lacking two predicted PPR motifs (Ppr10ΔPPR-FLAG). Mitochondrial heat shock protein Hsp60 detected by anti-human mitochondrial matrix protein HSP60 Ab serves as a loading control. (**E** and **F**) Deletion of *ppr10* results in a rapid loss of cell viability. Cells were grown overnight in YES, diluted to an initial OD_{600} of 0.2 and grown for 84 h. At 12 h intervals, aliquots of the cultures were 10-fold serially diluted, and either spotted or plated onto YES plates. Plates were either photographed (**E**) or grown colonies counted to determine cell viability (**F**). The percentage of cell viability was calculated by normalization to the viability of cells at 12 h.

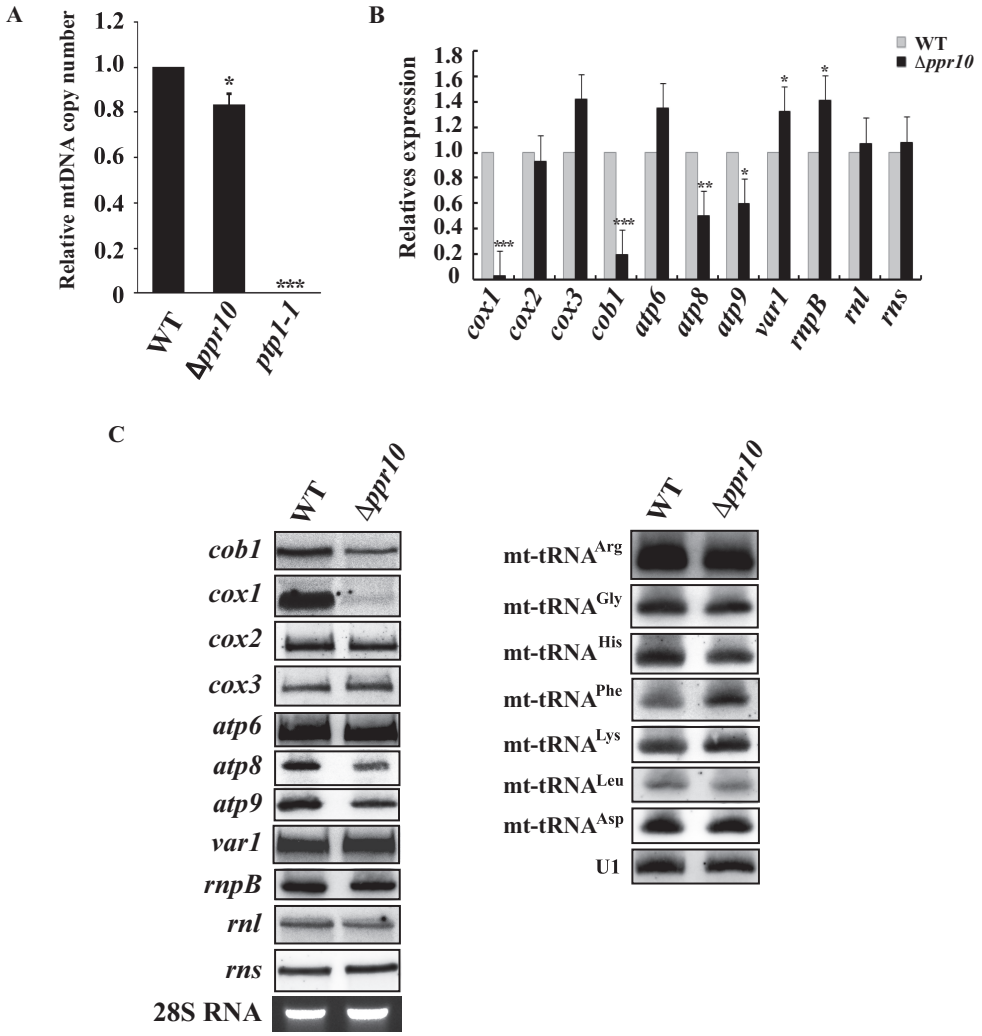

Figure 2. Analysis of mtDNA copy number and steady-state levels of mature mitochondrial-encoded RNAs (mt-RNAs) in wild-type (WT) and Δ*ppr10* cells. (**A**) mtDNA copy numbers in WT and Δ*ppr10* cells were measured by qPCR and expressed as mtDNA/nuclear DNA ratio. The fold change in mtDNA copy number of Δ*ppr10* cells compared to that of WT cells (whose value was set to 1) is shown. See Materials and Methods for details on the calculation. The error bars represent the S.D. of triplicates. Statistically significance was determined by the Student's *t*-test ($^{*}P < 0.05$, $^{***}P < 0.001$). As a control, mtDNA copy number in mtDNA-less *ptp1-1* cells was also measured. (**B**) qRT-PCR analysis of the steady-state levels of mature mt-RNAs in WT and Δ*ppr10* cells. Levels of mature mt-RNAs in Δ*ppr10* cells are normalized to the level of *htb1* mRNA and expressed as fold change over control WT strain yHL6381 (set to 1). Statistically significance was determined by the Student's *t*-test ($^{*}P < 0.05$, $^{**}P < 0.01$, $^{***}P < 0.001$). (**C**) Northern blot analysis of mature mt-RNAs from WT or Δ*ppr10* cells. Total RNAs were purified from WT or Δ*ppr10* cells, separated on a formaldehyde agarose gel or a denaturing polyacrylamide gel (7 M uera), transferred to a nylon membrane. The blots were hybridized with ^{32}P-labeled probes that specific for mt-RNAs as indicated. U1 snRNA detected by northern blotting and ethidium bromide-stained 28S rRNA were used as loading controls.

in the mt-tRNA 3′-end processing enzyme Trz2 (51). As shown in Figure 2C, the steady-state levels of all tRNAs analyzed were not significantly affected in Δ*ppr10* cells.

Ppr10 is required for mitochondrial translation

Next we examined the effect of *ppr10* deletion on mitochondrial protein synthesis. Mitochondrial translation products of WT and Δ*ppr10* cells were labeled with [^{35}S]-methionine/cysteine in the presence of the cytosolic translation inhibitor anisomycin. We used anisomycin because it gave a low background signal under our experimental conditions. For unknown reasons, *in vivo* labeling of mitochondrial proteins in *S. pombe* is much less efficient than in *S. cerevisiae* and human and requires a relatively long time (41,56). Nevertheless, the approach used here has been successfully used in *S. pombe* (41,61,65). Using this approach, we could identify all proteins synthesized by mitochondria based on their sizes and published results (41,61,65). As shown in Figure 3A, the levels of mtDNA-encoded proteins were substantially decreased in Δ*ppr10* cells compared to WT cells, indicating that *ppr10* is required for the synthesis of mtDNA-encoded proteins.

We next analyzed the effect of deletion of *ppr10* on the steady-state levels of mtDNA-encoded proteins by western blotting. We tried to generate anti-peptide Abs against all mtDNA-encoded proteins. However, only anti-peptide Abs against Cob1, Cox1, Cox2, Cox3 and Apt6 were able to recognize their target proteins. Analysis of mitochondrial pro-

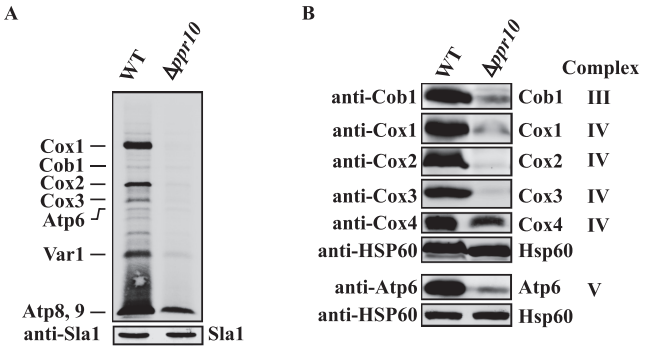

Figure 3. Deletion of *ppr10* impairs mitochondrial protein synthesis. (**A**) *In vivo* synthesis of mtDNA-encoded proteins in WT and Δ*ppr10* cells. Mitochondrial translation products were labeled by incubating cells with [^{35}S]-methionine/cysteine for 1.5 h in the presence of anisomycin. The labeled proteins were analyzed by sodium dodecyl sulphate-polyacrylamide gel electrophoresis (SDS-PAGE) and autoradiography. Sla1 detected by anti-Sla1 Ab serves as a loading control. Results presented are representative of multiple experiments. (**B**) Deletion of *ppr10* affects the steady state levels of mtDNA-encoded proteins. Mitochondrial extracts were prepared from WT and Δ*ppr10* cells by spheroplast lysis, and analyzed by western blotting with anti-peptide Abs against mitochondrial-encoded Cob1, Cox1, Cox2, Cox3 and Atp6, as well as nuclear-encoded Cox4. Hsp60 serves as a loading control.

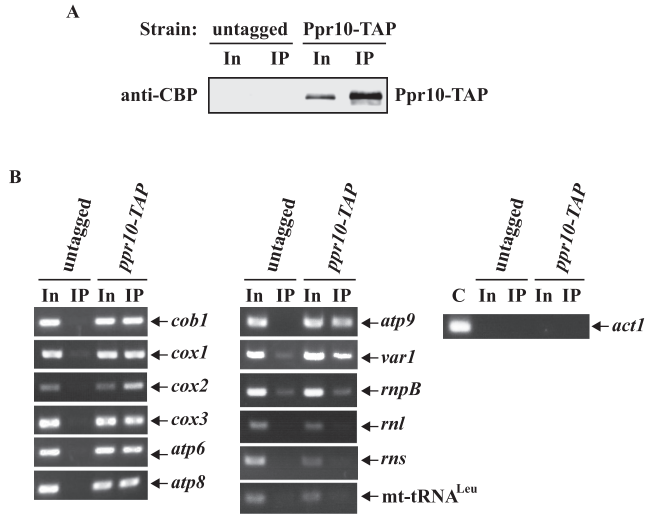

Figure 4. Ppr10 interacts with mt-mRNAs. Mitochondrial extracts prepared from *S. pombe* strains expressing chromosomally TAP-tagged *ppr10* and untagged *ppr10* (as a control) were immunoprecipitated with IgG agarose. (**A**) Western blot analysis. Mitochondrial extracts and immunoprecipitates (IP) were subjected to western blotting with anti-CBP Ab to detect Ppr10-TAP. Input (In) is 0.8% of total extract. (**B**) RT-PCR analysis. Total RNA was extracted from mitochondrial extracts (In) and the the IP and subjected to RT-PCR analysis with primers specific for mtDNA-encoded mRNAs, *rnpB*, *rnl*, *rns* and mt-tRNA^{Leu} and nuclear-encoded cytosolic *act1* mRNA. The RT-PCR bands of predicted sizes were cut out from agarose gels and sequenced to confirm that the observed RT-PCR products were derived from mt-RNAs. C: *act1* mRNA obtained by PCR from genomic DNA serves as a positive control.

tein extracts prepared from the Δ*ppr10* mutant and the isogenic WT strain using all available Abs revealed dramatic reductions in the protein levels of Cox1, Cox2, Cox3, Cob1 and Atp6 in the Δ*ppr10* mutant (Figure 3B). These results indicated that there was still residual synthesis of mtDNA-encoded proteins in the Δ*ppr10* mutant. We also examined the level of Cox4, a nuclear-encoded COX subunit, in the Δ*ppr10* mutant and found that the level of Cox4 was dramatically decreased in the mutant, suggesting reduced stability of the COX complex due to impairment of Cox1, Cox2 and Cox3 synthesis (Figure 3B).

Ppr10 is associated with mt-mRNAs

PPR proteins have been demonstrated to be associated with their target RNAs (11). To examine whether Ppr10 was physically associated with mt-RNAs using RIP assays, we first constructed a strain expressing a TAP tag integrated at the C-terminus of Ppr10 at its own genomic locus (Ppr10-TAP). This tag and additional tags described below did not apparently affect the *in vivo* function of the proteins, as assayed by growth on rich medium containing glycerol (Supplementary Figure S4A). In addition, all tagged proteins are of approximately the expected size (Supplementary Figure S4B). Ppr10 was immunociprecipitated from the mitochondrial extracts expressing Ppr10-TAP using IgG agarose beads (Figure 4A). RNA was purified from the total and immunoprecipitate fractions and analyzed by RT-PCR using primers specific for mt-mRNAs. To distinguish between Ppr10-TAP-associated RNA and RNA precipitated in a nonspecific way, untagged Ppr10 cells were used in parallel. The resulting RT-PCR products were sequenced to confirm their identities. RT-PCR analysis identified that mt-mRNAs but not mtDNA-encoded *rnpB*, rRNAs (*rnl* and *rns*) and tRNA^{Leu} were preferentially associated with Ppr10-TAP rather than with untagged Ppr10 (Figure 4B). As a control, nuclear-encoded cytosolic actin (*act1*) mRNA was not specifically immunoprecipitated by IgG agarose beads. These results indicate that Ppr10 may associate with all mtDNA-encoded mRNAs.

Ppr10 forms a complex with a novel protein called Mpa1 *in vivo* and interacts with Mpa1 *in vitro*

To identify Ppr10-interacting proteins, which might provide clues to understand the functions of Ppr10, we purified Ppr10-TAP using the TAP method and analyzed the proteins associated with Ppr10 by mass spectrometry. This analysis identified SPAPB1E7.11c as the top candidate that interacts with Ppr10 (Supplementary Table S3). As a negative control, MS analysis did not detect this protein when a parallel purification was performed using the extract from cells expressing Ppr2-TAP. We named this protein mitochondrial Ppr10-associated protein 1 (Mpa1).

Like *ppr10*, *mpa1* is assigned as non-essential in PomBase based on a genome-wide gene deletion analysis (66). The *mpa1* gene contains one intron within the 5′-UTR and encodes a 319 amino acid protein with a predicted molecular mass of 36.7 kDa. Mpa1 is annotated by PomBase as an orphan protein of unknown function. This protein is predicted by PomBase to contain a Rabaptin coiled-coil domain (^{116}EEGATKENEDFINEKEEEEDLS^{137}). Besides this domain, no other known protein domains could be identified in this protein. Secondary structure prediction for Mpa1 using PSIPRED shows that Mpa1 contains 32% α-

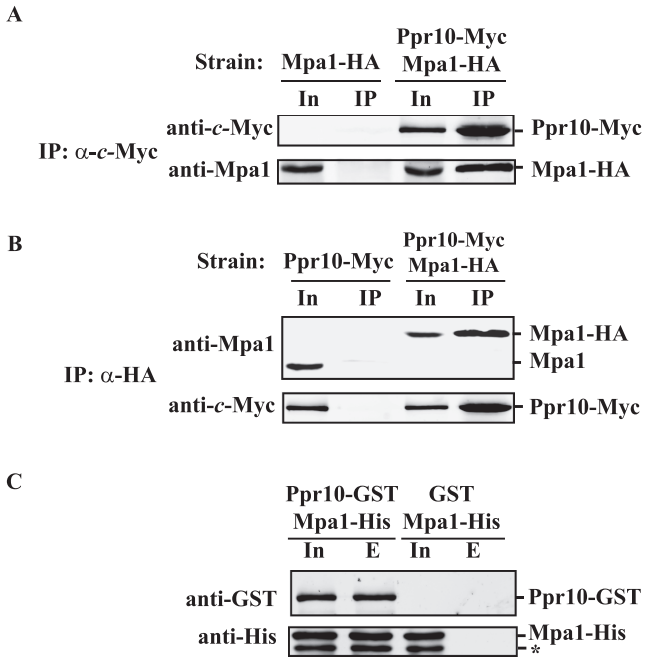

Figure 5. Ppr10 interacts with Mpa1 both *in vivo* and *in vitro*. (**A**) Co-immunoprecipitation (co-IP) of Ppr10 with Mpa1. Cells expressing chromosomally encoded Ppr10-Myc and Mpa1-HA were grown to mid-log phase in YES medium, lysed by glass bead beating and subjected to anti-*c*-Myc IPs. Extracts and IP were analyzed by western blotting with indicated Abs. 4% of the input extract (In) was run to show the expression level of each protein. An extract from WT cells expressing untagged Ppr10 and chromosomally encoded Mpa1-HA was used as a control. (**B**) Reciprocal co-IP of Ppr10 and Mpa1. The same extract in (A) was subjected to anti-HA IPs. Extracts and immunoprecipitates were analyzed by western blotting with indicated Abs. The amount of input (In) is 4% of the lysate used for IP. As a control, IP was performed on an extract from WT cells expressing untagged Mpa1 and chromosomally encoded Ppr10-Myc. (**C**) Ppr10 directly interacts with Mpa1. *E. coli* extracts expressing Ppr10-GST and Mpa1-His or GST and Mpa1-His were incubated with glutathione resin. Input (In, 3% of total protein) and proteins bound to GST (lane E) were analyzed by western blotting. The asterisk depicts a degradation product from Mpa1.

helices, 18% β-sheets and 50% loops (Supplementary Figure S5).

To corroborate the interaction between Ppr10 and Mpa1 *in vivo*, we performed co-IP experiments and analyzed the immunoprecipitates and whole-cell extracts by western blotting. Both Ppr10-Myc and Mpa1-HA were detectable in the anti-*c*-Myc immunoprecipitates obtained from cells expressing Ppr10-Myc and Mpa1-HA from their own promoters, but not from cells expressing Mpa1-HA and untagged Ppr10 (Figure 5A). In a reciprocal IP, both Ppr10-Myc and Mpa1-HA were detected in the anti-HA immunoprecipitates from the same above extract, but neither protein was detected by IP from extracts expressing Ppr10-Myc and untagged Mpa1 (Figure 5B). We also carried out IP using RNase A-treated whole-cell lysates. RNase A treatment did not abolish the interaction between Ppr10 and Mpa1 (Supplementary Figure S6). These data indicate that Ppr10 and Mpa1 associate with each other *in vivo* in an RNA-independent manner.

We next examined whether Ppr10 could directly interact with Mpa1 by performing *in vitro* pull-down assays. We tried bacterial and yeast expression systems to obtain recombinant Ppr10-GST fusion protein but failed, perhaps due to the extremely low level of Ppr10-GST expression. To circumvent the need for soluble recombinant Ppr10-GST, we carried out a GST-pull-down experiment using the supernatants of *E. coli* lysates co-expressing N-terminally GST-tagged Ppr10 (Ppr10-GST) and C-terminally 6His-tagged Mpa1 (Mpa1-His). We found that Mpa1-His could be pulled down by Ppr10-GST (Figure 5C). As a negative control, GST alone could not pull down Mpa1-His (Figure 5C). This suggest that Ppr10 directly interacts with Mpa1 and that coexpression with Mpa1 may improve the solubility of Ppr10.

Endogenous Ppr10 and Mpa1 are primarily soluble mitochondrial matrix proteins

A previous genome-wide analysis of protein subcellular localization using enhanced green fluorescent protein fusions failed to reveal the localization of Ppr10 and Mpa1 (67). Moreover, although Ppr10 contains a predicted 23-aa N-terminal mitochondrial targeting sequence, the mitochondrial targeting sequence of Mpa1 could not be identified using different subcellular localization prediction programs including MITOPROT (http://ihg.gsf.de/ihg/mitoprot.html) PSORT II (http://psort.hgc.jp/form2.html) Protein Prowler (http://bioinf.scmb.uq.edu.au:8080/pprowler_webapp_1-2/). To determine the localization of Ppr10 and Mpa1, mitochondria were isolated from cells expressing Ppr10-Myc and Mpa1-HA under the control of their own promoters, and the mitochondrial extracts were probed by western blotting for Ppr10-Myc and Mpa1-HA. As shown in Figure 6A, both Ppr10 and Mpa1 were found in the mitochondria-enriched fraction. As controls, the purified mitochondria are devoid of nuclear protein Sla1 (59) and contains mitochondrial protein Trz2 (51).

To further define the submitochondrial localization of Ppr10 and Mpa1, we followed procedures described previously. First, to determine whether Ppr10 and Mpa1 reside in the outer membrane, we treated mitochondrial preparation with proteinase K together with the detergent Triton X-100, which lyses both mitochondrial membranes. Protease treatment significantly reduced the level of Tom20-FLAG (Figure 6B), a mitochondrial outer membrane protein, but had little effect on the level of Ppr10-Myc and Mpa1-HA, suggesting that these two proteins reside within the mitochondria. Second, we subjected purified mitochondria to alkali treatment which can separate soluble and peripheral membrane proteins from integral membrane proteins (55). Both Ppr10 and Mpa1, like the mitochondrial matrix protein Hsp60 (SPAC12G12.04), were detected in the soluble fraction of sodium-carbonate-treated mitochondria (Figure 6C). All together, these results suggest that these two proteins are located in the mitochondrial matrix.

The *mpa1* deletion mutant exhibits growth defects reflecting reduced respiration

To examine the function of *mpa1 in vivo*, we generated a deletion mutant of *mpa1* and tested whether deletion of *mpa1* affected cell growth on different media. Like the

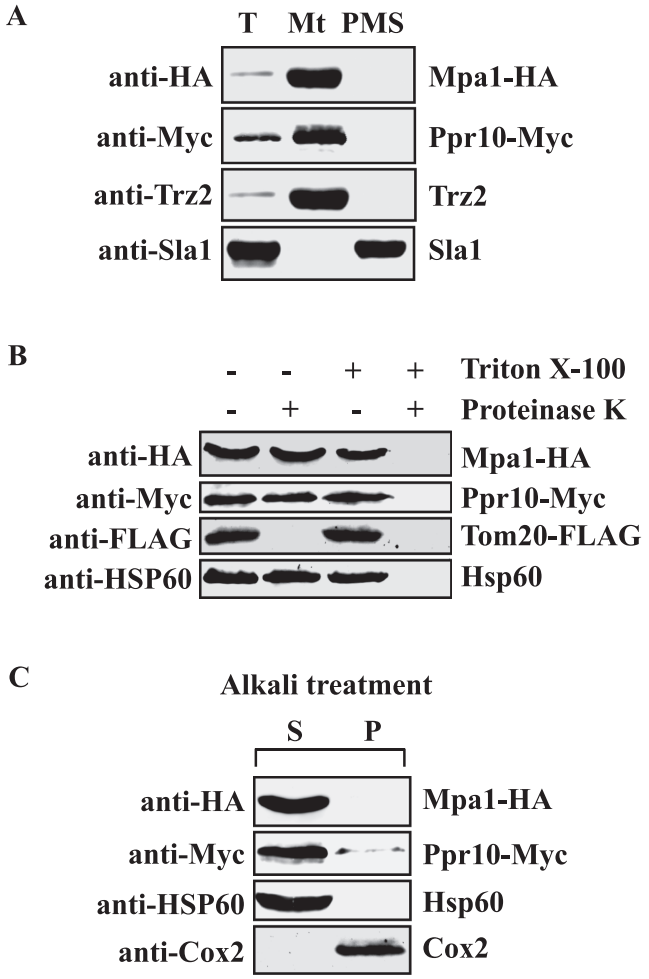

Figure 6. Ppr10 and Mpa1 are colocalized in the mitochondrial matrix. (**A**) Ppr10 is localized in mitochondria. Mitochondria were isolated from cells expressing Ppr10-Myc and Mpa1-HA as described in Materials and Methods. Total cell extracts (T), mitochondria (Mt) and postmitochondrial supernatants (PMS) were analyzed by western blotting using anti-HA Ab to detect Mpa1-HA, anti-*c*-Myc Ab to detect Ppr10-Myc, anti-Trz2 and anti-Sla1 Abs. Trz2 is a mitochondrial protein; Sla1 is a nuclear marker. (**B**) Ppr10-Myc is protected against proteinase K in mitochondrial fractions. Isolated mitochondria were treated with proteinase K in the absence or presence of Triton X-100 as indicated. After precipitation with tricarboxylic acid, samples were analyzed by immunoblot analysis using anti-HA, anti-*c*-Myc, anti-FLAG and anti-HSP60 Abs. (**C**) Alkali treatment of mitochondria. Purified mitochondria were extracted with 0.1 M sodium carbonate, pH ∼11.5. After centrifugation, soluble proteins (Supernatant, S) and the membrane-bound proteins (Pellet, P) were analyzed by SDS-PAGE and western blotting for Mpa1-HA, Ppr10-Myc, the mitochondrial matrix protein Hsp60 and the mitochondrial inner membrane protein Cox2.

Δ*ppr10* mutant, the Δ*mpa1* mutant grew slowly on glucose-containing YES medium but grew very slowly or not at all on glycerol- or galactose-containing rich media (Figure 7A). To determine whether a genetic interaction exists between *ppr10* and *mpa1*, we deleted these two genes individually or in combination and tested the ability of the resulting strains to use different carbon sources. The double mutant showed growth defects that are very similar to those of the single mutants, indicating that *ppr10* and *mpa1* did not have a synthetic genetic interaction on rich media (Figure 7A).

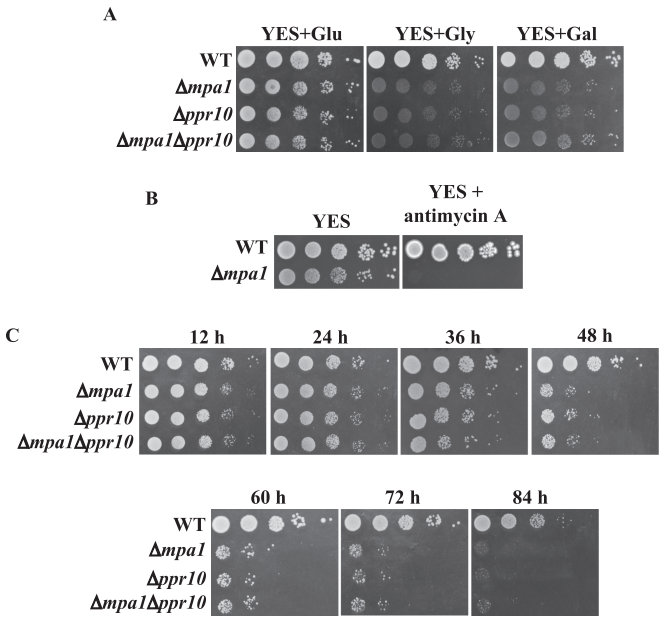

Figure 7. *mpa1* is required for respiratory growth of *S. pombe.* (**A**) Deletion of *mpa1* results in slow growth on YES medium, and failure to grow on non-fermentable carbon sources. The Δ*mpa1* mutant does not exhibit synthetic growth defects with the Δ*ppr10* mutant. Experiments were performed as in Figure 1A. (**B**) Loss of *mpa1* renders cells extraordinarily sensitive to antimycin A. The experiments were performed as in Figure 1B. (**C**) *mpa1* is required for cell survival in stationary phase. The experiments were performed as in Figure 1E.

Like the Δ*ppr10* mutant, the Δ*mpa1* mutant was extremely sensitive to antimycin A (Figure 7B) and lost viability much faster than the WT at late-station phase (Figure 7C). The cell viability of the Δ*ppr10* Δ*mpa1* double mutant is similar to both single mutant, indicating no genetic interaction between *ppr10* and *mpa1* (Figure 7C). Like Δ*ppr10* cells, Δ*mpa1* cells flocculate (Supplementary Figure S7). Together, these results indicate that the Δ*mpa1* mutant is defective in mitochondrial respiration.

Mpa1 is required for translation of mtDNA-encoded proteins

To understand the role of Mpa1, we first analyzed mtDNA copy number in Δ*mpa1* cells by qPCR. As shown in Figure 8A, mtDNA copy number in Δ*mpa1* cells was reduced to ∼88% of that in the WT strain, which is comparable to that in Δ*ppr10* cells. This result indicates that deletion of *mpa1* moderately reduces mtDNA copy number, but does not lead to depletion of mtDNA.

We next evaluated whether *mpa1* deletion affected the steady-state levels of mt-mRNAs by qRT-PCR and found that like the situation of *ppr10* deletion, only the levels of mature *cox1*, *cob1*, *atp8* and *atp9* mRNAs were reduced by *mpa1* deletion (Figure 8B). *cox1* mRNA shows a much more dramatic decline than other mRNAs in mRNA levels. These results were confirmed by northern blot analysis (Figure 8C). We also examined the effect of *mpa1* deletion on mitochondrial protein synthesis. Similar to *ppr10* deletion, *mpa1* deletion caused a general decrease in synthesis of mtDNA-encoded proteins (Figure 8D). Accordingly,

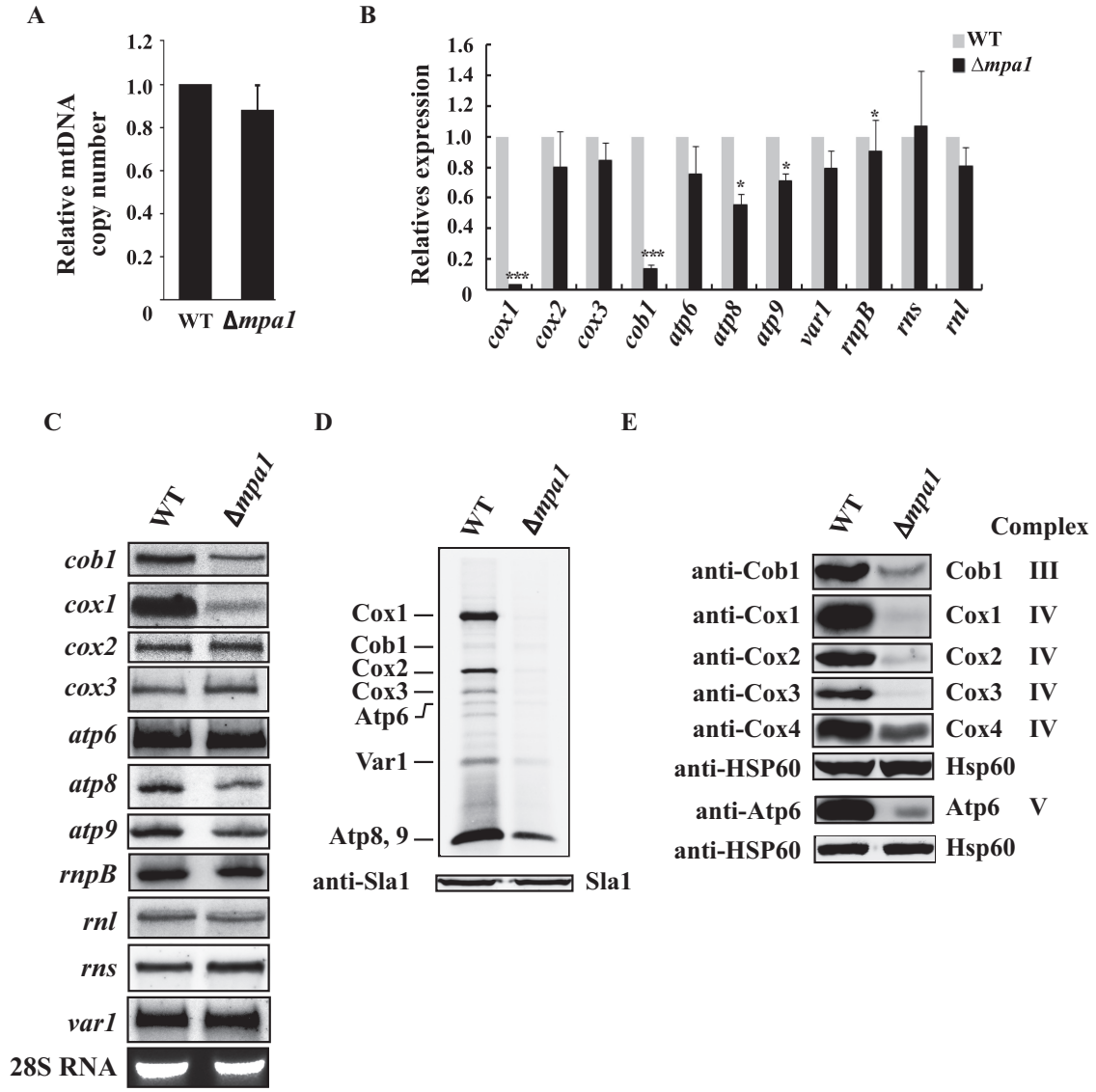

Figure 8. Analysis of mtDNA copy number, steady-state levels of mature mt-RNAs and mitochondrial protein synthesis in WT and Δ*mpa1* cells. (**A**) Determination of mtDNA copy numbers in WT and Δ*mpa1* cells by qPCR. (**B**) qRT-PCR analysis of the steady-state levels of mt-RNAs in WT and Δ*mpa1* cells. (**C**) Northern blot analysis of mature mt-RNAs from WT and Δ*mpa1* cells. (**D**) *In vivo* labeling of mitochondrial translation products with [^{35}S]-methionine/cysteine. (**E**) Deletion of *mpa1* affects steady-state mtDNA-encoded protein levels. The experiments were performed as in Figures 2 and 3.

steady-state levels of mtDNA-encoded proteins that have been tested were markedly reduced in the Δ*mpa1* mutant (Figure 8E).

Mpa1 maintains normal Ppr10 protein levels by preventing its degradation

Because the Δ*mpa1* mutant phenotypes were similar to those of the Δ*ppr10* mutant, it was very likely that disruption of *mpa1* may compromise Ppr10 function, or vice versa. We asked whether the Ppr10 protein levels were reduced in the absence of Mpa1. We found by using western blot analysis that the Δ*mpa1* mutant has lower protein levels of Ppr10 at all time points examined, and that these levels were 3- to 9-fold lower than those from the isogenic WT strain (Figure 9A). The Ppr10 protein levels in the Δ*mpa1* mutant were fully restored by exogenous expressing of WT Mpa1 (Figure 9B). By contrast, deletion of *ppr10* did not affected Mpa1 protein levels at all time points examined (Figure 9C).

To understand how deletion of *mpa1* leads to reduced the Ppr10 protein level, we first examined whether loss of *mpa1* affected the *ppr10* mRNA level by qRT-PCR. This analysis revealed that there was no significant change in the *ppr10* mRNA level in the absence of *mpa1* (Supplementary Figure S8), suggesting that Mpa1 is not involved in the transcription and stability of the *ppr10* mRNA and that the reduced level of the Ppr10 protein is most likely due to degradation of the protein. In *S. pombe*, there are three putative mitochondrial proteases Lon1 (SPAC22F3.06c), Yme1 (SPCC965.04c) and Yta12 (SPBC543.09) responsible for mitochondrial protein turnover. A possible candidate for

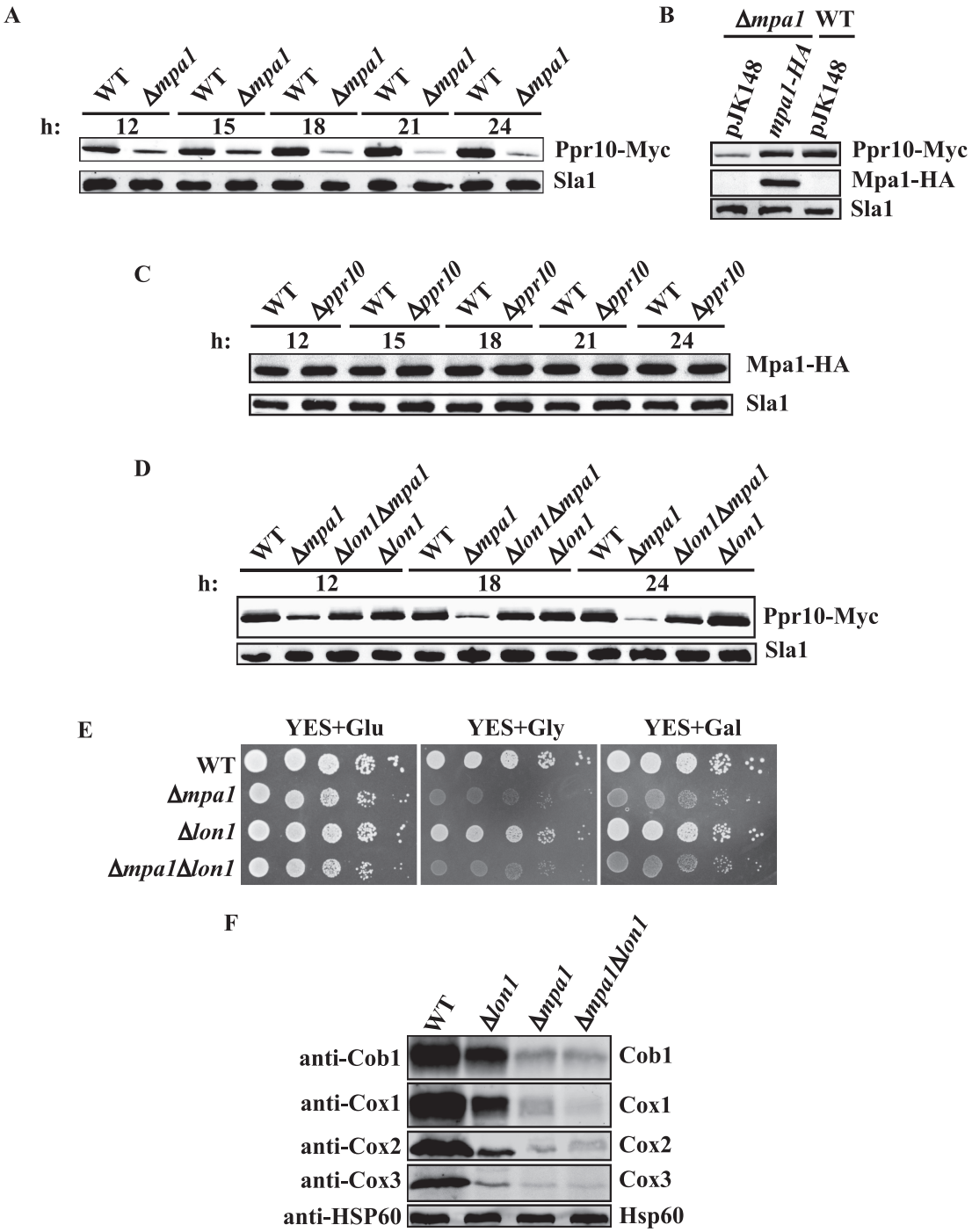

Figure 9. Mpa1 prevents Ppr10 degradation by Lon1. (**A**) Deletion of *mpa1* reduces Ppr10 protein levels. WT and Δ*mpa1* cells expressing chromosomally 13Myc-tagged Ppr10 were grown for the indicated time points (in hours), and the Ppr10 protein levels were monitored by western blotting with anti-*c*-Myc Ab. The results are representative of three independent experiments. (**B**) Reduction of Ppr10 protein levels by *mpa1* deletion can be rescued by expression of WT Mpa1. Δ*mpa1* cells expressing chromosomally 13Myc-tagged Ppr10 were transformed with an integrated empty vector pJK148 or an integrated vector expressing 3HA-tagged Mpa1 under the control of its native promoter, and WT cells expressing chromosomally 13Myc-tagged Ppr10 were transformed with pJK148. Cells were grown for 18 h. Ppr10 protein levels were visualized by western blotting with anti-*c*-Myc Ab. (**C**) The Mpa1 protein levels are not affected in the absence of Ppr10. WT and Δ*ppr10* cells expressing chromosomally 3HA-tagged Mpa1 were grown for the indicated time points, and the Mpa1 protein levels were monitored by western blotting with anti-HA Ab. (**D**) Deletion of *lon1* restores the Ppr10 protein levels. WT, Δ*mpa1*, Δ*lon1* and Δ*mpa1*Δ*lon1* cells expressing chromosomally encoded 13Myc-tagged Ppr10 were grown for the indicated times, and Ppr10 protein levels were monitored by western blotting with anti-*c*-Myc Ab. For A–D, extracts were prepared by alkaline extraction. Sla1 serves as a loading control. (**E**) Deletion of *lon1* cannot rescue the respiratory growth defect of Δ*mpa1* cells. A 10-fold dilution spot assay of cells were spotted on YES+Glu, YES+Gly or YES+Gal and incubated at 30°C. (**F**) Deletion of *lon1* cannot restore the protein levels of mitochondrial-encoded proteins. Mitochondrial extracts were prepared from WT, Δ*lon1*, Δ*mpa1* and Δ*lon1*Δ*mpa1* cells by spheroplast lysis, and analyzed by western blotting using anti-Cob1, Cox1, Cox2 and Cox3 Abs. Hsp60 serves as a loading control.

Ppr10 degradation is Lon1, because the Lon protease is the main protease responsible for the degradation of soluble mitochondrial matrix proteins in *S. cerevisiae* and humans (68–70). Therefore, we next examined whether *lon1* is involved in degradation of Ppr10. The result demonstrated that the Ppr10 protein levels were restored nearly to the WT levels in the Δ*lon1*Δ*mpa1* double mutant (Figure 9D). We also examined whether the respiration growth defect of the Δ*mpa1* mutant could be rescued by deletion of *lon1*. Spotting assays showed that Δ*lon1* cells grew slightly slower than WT cells on both fermentable and non-fermentable carbon sources. However, the Δ*lon1*Δ*mpa1* double mutant could not grow on rich medium containing glycerol or galactose (Figure 9E). We further tested whether *lon1* deletion would restore the levels of the mtDNA-encoded proteins by western blot analysis. In *S. cerevisiae*, the Lon protease PIM1 is required for proper expression of intron-containing genes in mitochondria (71). As expected, deletion of *lon1* resulted in reduced steady-state protein levels of Cob1, Cox1, Cox2 and Cox3 (Figure 9F). Importantly, in the Δ*lon1*Δ*mpa1* double mutant, the protein levels of mitochondrial-encoded proteins could not be restored to levels observed in the Δ*lon1* mutant. These results demonstrate that the restoration of normal protein levels of Ppr10 by *lon1* deletion is not sufficient to suppress the respiratory growth defect of the Δ*mpa1* mutant.

Ppr10 associates with the putative mitochondrial translation initiation factor Mti2

Because Ppr10 is required for mitochondrial translation and PPR proteins are strongly thought to play a role in translation initiation, we examined whether Ppr10 interacts with mitochondrial translation initiation factors. There are currently two putative mitochondrial translation initiation factors Mti2 (SPBC1271.15c) and Mti3 (SPBC18E5.13) annotated in PomBase. We constructed two strains: one expressing 13Myc-tagged Ppr10 and 2FLAG-tagged Mti2 and a second one expressing 13Myc-tagged Ppr10 and 2FLAG-tagged Mti3. We performed IP experiments using anti-*c*-Myc Ab against Ppr10-Myc. Proteins associated with anti-*c*-Myc immunoprecipitates were analyzed by western blotting with anti-FLAG Ab to detect Mti2-FLAG or Mti3-FLAG. Western blot analysis demonstrated that Mti2-FLAG but not Mti3-FLAG could be co-immunoprecipitated with Ppr10-Myc (Figure 10A and B). RNase A treatment did not abolish the interaction between Ppr10-Myc and Mti2-FLAG, indicating that the interaction between these two proteins does not dependent on RNA (Supplementary Figure S9). However, reciprocal IP of Mti2 followed by western blotting with anti-*c*-Myc Ab failed to detect the presence of Ppr10. Two possible reasons for this failure are (i) only a small portion of Mti2 is associated with Ppr10 or (ii) the association between Ppr10 and Mti2 masks the *c*-Myc epitope on the Mti2 C-terminus.

To examine whether Ppr10 could directly interact with Mti2 or Mti3, we performed *in vitro* pull-down assays as described above for Ppr10 and Mpa1. GST pull-down assays were performed using lysates of *E. coli* cells co-expressing GST tagged Ppr10 (Ppr10-GST) with either His-tagged Mti2 (Mti2-His) or His-tagged Mti3 (Mti3-His). As controls, GST pull-down assays were also performed using lysates of *E. coli* cells co-expressing the GST protein with either Mti2-His or Mti3-His. As shown in Figure 10C and D, Mti2-His was pulled down with glutathione resin bound to Ppr10-GST but not control GST whereas Mti3-His could not be pulled down by Ppr10-GST, suggesting that Mti2 but not Mti3 specifically interacts with Ppr10.

DISCUSSION

In this study, we first characterized a putative *S. pombe* PPR protein Ppr10. Like most other *S. pombe* PPR proteins, Ppr10 is annotated as a *Schizosaccharomyces*-specific protein in PomBase. The PPR motifs of *S. pombe* are usually highly degenerate, making them difficult to identify. The PPR protein characterized in this work was not identified in a previous genome-wide search for *S. pombe* PPR proteins (41), likely due to higher degrees of degeneracy of its PPR motifs. In addition, Ppr10 appears to contain the smallest number of PPR motifs predicted by TPRpred. However, it may contain additional more highly degenerate PPR motifs as suggested by the secondary structure prediction of Ppr10. Although further work is needed to verify these putative motifs, we demonstrate that the predicted PPR motifs found in Ppr10 are necessary for respiratory function.

The Δ*ppr10* mutant, like other *ppr* deletion mutants, exhibits defective respiratory growth, as assessed by growth on the non-fermentable carbon sources. In addition, like some *ppr* deletion mutants, Δ*ppr10* cells flocculate considerably. It remains to be determined why among *ppr* deletion mutants, some flocculate, whereas others do not. Δ*ppr10* cells are significantly more sensitive than the WT strain to antimycin A, shared by some but not all other *ppr* deletion mutants. It should be noted that although both Ppr10 and the previously characterized Ppr2 appear to be general mitochondrial translation factors (see below Discussion), the Δ*ppr10* mutant has phenotypes that are quite distinct from the Δ*ppr2* mutant. For example, unlike Δ*ppr2* cells, which are modestly sensitive to antimycin A and flocculate slightly, cells of Δ*ppr10* show an increased sensitivity to antimycin A and flocculate strongly in YES medium. In addition, Ppr10 is primarily localized in the mitochondrial matrix, whereas Ppr2 is located mainly on the mitochondrial membrane (41).

Δ*ppr10* cells have reduced viability during prolonged stationary phase growth in rich glucose medium and therefore a shortened chronological life span. This phenotype has also been observed in other respiration-deficient mutants that have increased levels of reactive oxygen species (ROS) (63). As described elsewhere (72), we have recently shown that loss of *ppr3*, *ppr4*, *ppr6* or *ppr10* perturbs iron homeostasis and leads to enhanced ROS production and apoptotic cell death in *S. pombe*.

Deletion of *ppr10* induces only mild loss of mtDNA. qRT-PCR and northern blotting reveals that deletion of *ppr10* causes reductions in the levels of *cox1*, *cob1*, *atp8* and *atp9* mRNAs to varying degrees. The levels of other mtRNAs were not appreciably affected by *ppr10* deletion. It is possible that *ppr10* is required for the stability or production of the *cox1*, *cob1*, *atp8* and *atp9* mRNAs.

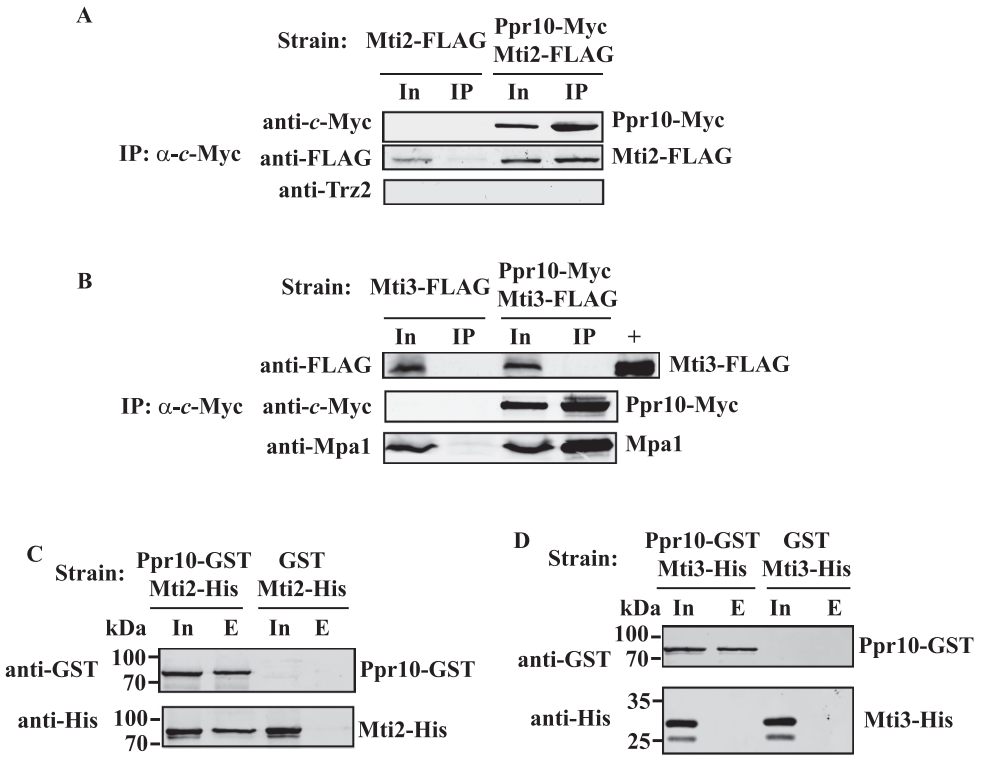

Figure 10. Ppr10 interacts with Mti2 but not with Mti3 *invivo* and *invitro*. (**A** and **B**) Ppr10 co-immunoprecipitates with Mti2, but not with Mti3. Extracts of cells expressing chromosomally encoded (**A**) Ppr10-Myc and Mti2-FLAG or (**B**) Ppr10-Myc and Mti3-FLAG were used for IP with anti-*c*-Myc agarose beads. Control IPs were also performed on extracts of cells expressing chromosomally encoded (A) Mti2-FLAG or (B) Mti3-FLAG. Extracts were prepared by glass bead disruption. IPs were performed in the same way as described in Figure 5, except that the beads were washed under moderate stringent conditions to prevent dissociation of weakly bound proteins (see Materials and Methods for details). Extracts and IPs were subjected to western blotting with indicated Abs. Input (In) lanes contain 4% of the extracts used for IP. Lane + contains affinity purified Mti3-FLAG served as the positive control. Anti-Mpa1 Ab was used as a positive control. (**C** and **D**) Ppr10 pulls down Mti2, but not Mti3. Whole cell lysates of *E. coli* cells co-expressing GST or Ppr10-GST with (**C**) Mti2-His, or (**D**) Mti3-His were incubated with glutathione resin, and proteins bound to GST were analyzed by western blotting with anti-GST and anti-His Abs. In, Input (1% of total protein), E, bound proteins.

The *cox1* mRNA is the most severely affected mt-mRNA in Δ*ppr10* cells, followed by the *cob1* mRNA. The reason for this is unknown. One possible explanation for this result is as follows: Among mtDNA-encoded genes, only the *cob1* and *cox1* genes contain introns. These two genes have, respectively, one and two introns. Some of these introns encode mRNA maturases required for the removal of introns from the *cox1* and *cob1* transcripts. Thus, it is likely that the synthesis of these maturases are impaired by the defective mitochondrial translation caused by *ppr10* deletion, leading to a dramatic reduction of mature *cox1* and *cob1* mRNAs. In particular, the level of the mature *cox1* mRNA is barely detectable in Δ*ppr10* cells. It has been shown that deletion of *S. pombe ppr4* or *ppr8* individually results in the absence of mature *cox1* mRNA in the background of intron-containing mtDNA but not in the background of intronless mtDNA (41). In *S. cerevisiae*, the *pet309* deficiency abolishes mature *COX1* RNA accumulation in the background of intron-containing mtDNA (24). However, in the background of intronless mtDNA, the deficiency of *pet309* does not affect accumulation of mature *COX1* RNA (24).

Analysis of mitochondrial translation products and the steady-state levels of mtDNA-encoded proteins in Δ*ppr10* cells reveals considerably impaired translation of all mtDNA-encoded proteins. The impaired translation of the *cox1*, *cob1*, *atp8* and *atp9* mRNAs can be explained by reductions in accumulated levels of their mRNA levels. However, the role of Ppr10 in stability or production of the *cox1*, *cob1*, *atp8* and *atp9* mRNAs does not exclude the possibility that Ppr10 plays a role in the translation of these mt-mRNAs. Furthermore, the levels of all other mt-mRNAs are not affected by *ppr10* deletion. It is very likely that Ppr10 plays a general role in mitochondrial translation. This hypothesis is further supported by our findings that Ppr10 associates with all mt-mRNAs and that Ppr10 interacts with the putative mitochondrial translation initiation factor Mti2 *in vitro* and *in vivo*.

Although we have shown that mt-mRNAs can be specifically precipitated by co-IP with Ppr10, it remains to determine the nature of the association of Ppr10 with mt-mRNAs and how Ppr10 activates their translation. Because PPR motifs have been shown to bind RNA, with one PPR motif interacting with one RNA base, it is possible that Ppr10 may directly interact with mt-mRNAs through its PPR motifs, and facilitate their association with the mitochondrial translational machinery. However, it is also possible that Ppr10 may indirectly associate with mt-mRNAs. The precipitated mt-mRNAs may not be derived from Ppr10 but from its binding partner Mpa1, another co-factor or the component(s) of the mitochondrial transla-

tional machinery. Further work will be required to distinguish between these two possibilities.

In this study, we identified Mpa1 as a novel protein interacting partner for Ppr10 in fission yeast. Further characterization of the interaction between these two proteins will be described elsewhere. So far, only a few interacting partners of PPR proteins have been identified. The rice PPR proteins RF5 and RF6, which are required for the processing of the cytoplasmic male sterility-associated transcripts and restoration of fertility, interact with GRP162 and hexokinase 6, respectively (73,74). In the flowering plants, PPR proteins interact with MORF proteins (also called RIP proteins) to form the plant organellar RNA editing apparatus (75–81). The human, mouse and *Drosophila* LRPPRC interacts with SLIRP (36–38,82). The identification of a growing number of binding partners of PPR proteins suggests that PPR proteins may require binding partners to fulfill their functions.

Deletion of *mpa1* results in phenotypes very similar to those seen in the Δ*ppr10* mutant. In addition, we did not observe any specific genetic interaction between Δ*ppr10* and Δ *mpa1*. These results suggest that the phenotypes of the Δ*mpa1* mutant might be caused by a reduction in either the level of *ppr10* expression or Ppr10 protein stability. Since there is no change in *ppr10* mRNA levels in the absence of *mpa1*, it is most likely that Mpa1 stabilizes Ppr10 by preventing it from degradation. Indeed, the absence of mitochondrial matrix protease gene *lon1* results in nearly WT levels of the Ppr10 protein. However, deletion of *lon1* cannot rescue the respiratory defect of the Δ*mpa1* mutant. Thus, it is reasonable to speculate that, besides protecting Ppr10 from degradation, Mpa1 may also enhance its proper folding and/or stabilize its interaction with target RNAs. As mentioned above, it is also possible that Mpa1 may directly bind mt-mRNAs.

Our study reveals that the stability of Ppr10 is affected by its interacting partner Mpa1, suggesting that Ppr10 has low stability. This property appears to be common to many PPR proteins. Although close homologs of these two proteins are limited to *Schizosaccharomyces* species, protein stabilization through protein–protein interaction is also observed for mammalian LRPPRC/SLIRP, suggestive of a common mechanism by which PPR proteins may achieve stability. Deletion of mouse *SLIRP* reduces the protein levels of LRPPRC down to about 25% of WT levels (68). SLIRP stabilizes LRPPRC by preventing it from being targeted for degradation by the Lon protease LONP1 (68) and by preventing formation of larger LRPPRC oligomers or aggregates (83). However, unlike the situation in *S. pombe*, where *ppr10* deletion does not compromise the stability of Mpa1, conditional knockout of *LRPPRC* in mice results in a complete loss of SLIRP, indicating that the two mouse proteins stabilize each other (37).

SUPPLEMENTARY DATA

Supplementary Data are available at NAR Online.

ACKNOWLEDGEMENTS

The authors thank Juraj Gregan, Thomas D. Fox, Christopher J. Herbert, Antoni Barrientos, Nathalie Bonnefoy, Jianhua Liu, Zhaoqing Chu, Valerie Wood and Ling Lu for reagents and helpful discussion and Fei Chen, Ping Wang, Hua Huang and Jinjie Shang for technical assistance.
Authors' contributions: Y.W., J.Y., Q.Z., X.M., J.Z., M.S. performed the experiments and analyzed the data. Y.H. conceived this study, analyzed the data and drafted the manuscript. All authors have read and approved the final version of the manuscript.

FUNDING

National Natural Science Foundation of China [31470778 to Y.H.]; Priority Academic Program Development of Jiangsu Higher Education Institutions (to Y.H.). Funding for open access charge: National Natural Science Foundation of China [31470778 to Y.H.]; Priority Academic Program Development of Jiangsu Higher Education Institutions (to Y.H.).
Conflict of interest statement. None declared.

REFERENCES

1. Green,D.R., Galluzzi,L. and Kroemer,G. (2014) Metabolic control of cell death. *Science*, **345**, 1250256.
2. Birsoy,K., Wang,T., Chen,W.W., Freinkman,E., Abu-Remaileh,M. and Sabatini,D.M. (2015) An essential role of the mitochondrial electron transport chain in cell proliferation is to enable aspartate synthesis. *Cell*, **162**, 540–551.
3. Sullivan,L.B., Gui,D.Y., Hosios,A.M., Bush,L.N., Freinkman,E. and Vander Heiden,M.G. (2015) Supporting aspartate biosynthesis is an essential function of respiration in proliferating cells. *Cell*, **162**, 552–563.
4 Kauppila,T.E., Kauppila,J.H. and Larsson,N.G. (2017) Mammalian mitochondria and aging: an update. *Cell Metab.*, **25**, 57–71.
5. Schafer,B. (2005) RNA maturation in mitochondria of *S. cerevisiae* and *S. pombe*. *Gene*, **354**, 80–85.
6. Barkan,A. and Small,I. (2014) Pentatricopeptide repeat proteins in plants. *Annu. Rev. Plant Biol.*, **65**, 415–442.
7. Herbert,C.J., Golik,P. and Bonnefoy,N. (2013) Yeast PPR proteins, watchdogs of mitochondrial gene expression. *RNA Biol.*, **10**, 1477–1494.
8. Lightowlers,R.N. and Chrzanowska-Lightowlers,Z.M. (2013) Human pentatricopeptide proteins: only a few and what do they do? *RNA Biol.*, **10**, 1433–1438.
9. Manna,S. (2015) An overview of pentatricopeptide repeat proteins and their applications. *Biochimie*, **113**, 93–99.
10. Schmitz-Linneweber,C. and Small,I. (2008) Pentatricopeptide repeat proteins: a socket set for organelle gene expression. *Trends Plant Sci.*, **13**, 663–670.
11. Zamudio-Ochoa,A., Camacho-Villasana,Y., Garcia-Guerrero,A.E. and Perez-Martinez,X. (2014) The Pet309 pentatricopeptide repeat motifs mediate efficient binding to the mitochondrial *COX1* transcript in yeast. *RNA Biol.*, **11**, 953–967.
12. Barkan,A., Rojas,M., Fujii,S., Yap,A., Chong,Y.S., Bond,C.S. and Small,I. (2012) A combinatorial amino acid code for RNA recognition by pentatricopeptide repeat proteins. *PLOS Genet.*, **8**, e1002910.
13. Takenaka,M., Zehrmann,A., Brennicke,A. and Graichen,K. (2013) Improved computational target site prediction for pentatricopeptide repeat RNA editing factors. *PLoS One*, **8**, e65343.
14. Yagi,Y., Hayashi,S., Kobayashi,K., Hirayama,T. and Nakamura,T. (2013) Elucidation of the RNA recognition code for pentatricopeptide repeat proteins involved in organelle RNA editing in plants. *PLoS One*, **8**, e57286.
15. Coquille,S., Filipovska,A., Chia,T., Rajappa,L., Lingford,J.P., Razif,M.F., Thore,S. and Rackham,O. (2014) An artificial PPR scaffold for programmable RNA recognition. *Nat. Commun.*, **5**, 5729.
16. Howard,M.J., Lim,W.H., Fierke,C.A. and Koutmos,M. (2012) Mitochondrial ribonuclease P structure provides insight into the

evolution of catalytic strategies for precursor-tRNA 5′ processing. *Proc. Natl. Acad. Sci. U.S.A.*, **109**, 16149–16154.
17. Yin,P., Li,Q., Yan,C., Liu,Y., Liu,J., Yu,F., Wang,Z., Long,J., He,J., Wang,H.W. *et al.* (2013) Structural basis for the modular recognition of single-stranded RNA by PPR proteins. *Nature*, **504**, 168–171.
18. Ringel,R., Sologub,M., Morozov,Y.I., Litonin,D., Cramer,P. and Temiakov,D. (2011) Structure of human mitochondrial RNA polymerase. *Nature*, **478**, 269–273.
19. Ban,T., Ke,J., Chen,R., Gu,X., Tan,M.H., Zhou,X.E., Kang,Y., Melcher,K., Zhu,J.K. and Xu,H.E. (2013) Structure of a PLS-class pentatricopeptide repeat protein provides insights into mechanism of RNA recognition. *J. Biol. Chem.*, **288**, 31540–31548.
20. Ke,J., Chen,R.Z., Ban,T., Zhou,X.E., Gu,X., Tan,M.H., Chen,C., Kang,Y., Brunzelle,J.S., Zhu,J.K. *et al.* (2013) Structural basis for RNA recognition by a dimeric PPR-protein complex. *Nat. Struct. Mol. Biol.*, **20**, 1377–1382.
21. Tavares-Carreon,F., Camacho-Villasana,Y., Zamudio-Ochoa,A., Shingu-Vazquez,M., Torres-Larios,A. and Perez-Martinez,X. (2008) The pentatricopeptide repeats present in Pet309 are necessary for translation but not for stability of the mitochondrial COX1 mRNA in yeast. *J. Biol. Chem.*, **283**, 1472–1479.
22. Costanzo,M.C. and Fox,T.D. (1988) Specific translational activation by nuclear gene products occurs in the 5′ untranslated leader of a yeast mitochondrial mRNA. *Proc. Natl. Acad. Sci. U.S.A.*, **85**, 2677–2681.
23. Green-Willms,N.S., Butler,C.A., Dunstan,H.M. and Fox,T.D. (2001) Pet111p, an inner membrane-bound translational activator that limits expression of the *Saccharomycescerevisiae* mitochondrial gene *COX2*. *J. Biol. Chem.*, **276**, 6392–6397.
24. Manthey,G.M. and McEwen,J.E. (1995) The product of the nuclear gene *PET309* is required for translation of mature mRNA and stability or production of intron-containing RNAs derived from the mitochondrial *COX1* locus of *Saccharomyces cerevisiae*. *EMBO J.*, **14**, 4031–4043.
25. Siep,M., van Oosterum,K., Neufeglise,H., van der Spek,H. and Grivell,L.A. (2000) Mss51p, a putative translational activator of cytochrome *c* oxidase subunit-1 (*COX1*) mRNA, is required for synthesis of Cox1p in *Saccharomyces cerevisiae*. *Curr. Genet.*, **37**, 213–220.
26. Roloff,G.A. and Henry,M.F. (2015) Mam33 promotes cytochrome *c* oxidase subunit I translation in *Saccharomyces cerevisiae* mitochondria. *Mol. Biol. Cell*, **26**, 2885–2894.
27. Poutre,C.G. and Fox,T.D. (1987) *PET111*, a *Saccharomyces cerevisiae* nuclear gene required for translation of the mitochondrial mRNA encoding cytochrome *c* oxidase subunit II. *Genetics*, **115**, 637–647.
28. Costanzo,M.C. and Fox,T.D. (1986) Product of *Saccharomyces cerevisiae* nuclear gene *PET494* activates translation of a specific mitochondrial mRNA. *Mol. Cell. Biol.*, **6**, 3694–3703.
29. Costanzo,M.C., Seaver,E.C. and Fox,T.D. (1986) At least two nuclear gene products are specifically required for translation of a single yeast mitochondrial mRNA. *EMBO J.*, **5**, 3637–3641.
30. Kloeckener-Gruissem,B., McEwen,J.E. and Poyton,R.O. (1988) Identification of a third nuclear protein-coding gene required specifically for posttranscriptional expression of the mitochondrial *COX3* gene is *Saccharomyces cerevisiae*. *J. Bacteriol.*, **170**, 1399–1402.
31. Wiesenberger,G., Costanzo,M.C. and Fox,T.D. (1995) Analysis of the *Saccharomyces cerevisiae* mitochondrial *COX3* mRNA 5′ untranslated leader: translational activation and mRNA processing. *Mol. Cell. Biol.*, **15**, 3291–3300.
32. Gruschke,S., Kehrein,K., Rompler,K., Grone,K., Israel,L., Imhof,A., Herrmann,J.M. and Ott,M. (2011) Cbp3-Cbp6 interacts with the yeast mitochondrial ribosomal tunnel exit and promotes cytochrome *b* synthesis and assembly. *J. Cell Biol.*, **193**, 1101–1114.
33. Fontanesi,F., Clemente,P. and Barrientos,A. (2011) Cox25 teams up with Mss51, Ssc1, and Cox14 to regulate mitochondrial cytochrome *c* oxidase subunit 1 expression and assembly in *Saccharomyces cerevisiae*. *J. Biol. Chem.*, **286**, 555–566.
34. Mootha,V.K., Lepage,P., Miller,K., Bunkenborg,J., Reich,M., Hjerrild,M., Delmonte,T., Villeneuve,A., Sladek,R., Xu,F. *et al.* (2003) Identification of a gene causing human cytochrome *c* oxidase deficiency by integrative genomics. *Proc. Natl. Acad. Sci. U.S.A.*, **100**, 605–610.
35. Xu,F., Morin,C., Mitchell,G., Ackerley,C. and Robinson,B.H. (2004) The role of the *LRPPRC* (leucine-rich pentatricopeptide repeat cassette) gene in cytochrome oxidase assembly: mutation causes lowered levels of COX (cytochrome *c* oxidase) I and COX III mRNA. *Biochem. J.*, **382**, 331–336.
36. Sasarman,F., Brunel-Guitton,C., Antonicka,H., Wai,T., Shoubridge,E.A. and Consortium,L. (2010) LRPPRC and SLIRP interact in a ribonucleoprotein complex that regulates posttranscriptional gene expression in mitochondria. *Mol. Biol. Cell*, **21**, 1315–1323.
37. Ruzzenente,B., Metodiev,M.D., Wredenberg,A., Bratic,A., Park,C.B., Camara,Y., Milenkovic,D., Zickermann,V., Wibom,R., Hultenby,K. *et al.* (2012) LRPPRC is necessary for polyadenylation and coordination of translation of mitochondrial mRNAs. *EMBO J.*, **31**, 443–456.
38. Chujo,T., Ohira,T., Sakaguchi,Y., Goshima,N., Nomura,N., Nagao,A. and Suzuki,T. (2012) LRPPRC/SLIRP suppresses PNPase-mediated mRNA decay and promotes polyadenylation in human mitochondria. *Nucleic Acids Res.*, **40**, 8033–8047.
39. Weraarpachai,W., Antonicka,H., Sasarman,F., Seeger,J., Schrank,B., Kolesar,J.E., Lochmuller,H., Chevrette,M., Kaufman,B.A., Horvath,R. *et al.* (2009) Mutation in *TACO1*, encoding a translational activator of COX I, results in cytochrome *c* oxidase deficiency and late-onset Leigh syndrome. *Nat. Genet.*, **41**, 833–837.
40. Richman,T.R., Spahr,H., Ermer,J.A., Davies,S.M., Viola,H.M., Bates,K.A., Papadimitriou,J., Hool,L.C., Rodger,J., Larsson,N.G. *et al.* (2016) Loss of the RNA-binding protein TACO1 causes late-onset mitochondrial dysfunction in mice. *Nat. Commun.*, **7**, 11884.
41. Kuhl,I., Dujeancourt,L., Gaisne,M., Herbert,C.J. and Bonnefoy,N. (2011) A genome wide study in fission yeast reveals nine PPR proteins that regulate mitochondrial gene expression. *Nucleic Acids Res.*, **39**, 8029–8041.
42. Rothstein,R.J. (1983) One-step gene disruption in yeast. *Methods Enzymol.*, **101**, 202–211.
43. Bahler,J., Wu,J.Q., Longtine,M.S., Shah,N.G., McKenzie,A. 3rd, Steever,A.B., Wach,A., Philippsen,P. and Pringle,J.R. (1998) Heterologous modules for efficient and versatile PCR-based gene targeting in *Schizosaccharomyces pombe*. *Yeast*, **14**, 943–951.
44. Cipak,L., Spirek,M., Novatchkova,M., Chen,Z., Rumpf,C., Lugmayr,W., Mechtler,K., Ammerer,G., Csaszar,E. and Gregan,J. (2009) An improved strategy for tandem affinity purification-tagging of *Schizosaccharomyces pombe* genes. *Proteomics*, **9**, 4825–4828.
45. Moreno,S., Klar,A. and Nurse,P. (1991) Molecular genetic analysis of fission yeast *Schizosaccharomyces pombe*. *Methods Enzymol.*, **194**, 795–823.
46. Keeney,J.B. and Boeke,J.D. (1994) Efficient targeted integration at *leu1-32* and *ura4-294* in *Schizosaccharomyces pombe*. *Genetics*, **136**, 849–856.
47. Forsburg,S.L. (1993) Comparison of *Schizosaccharomyces pombe* expression systems. *Nucleic Acids Res.*, **21**, 2955–2956.
48. Punt,P.J., Oliver,R.P., Dingemanse,M.A., Pouwels,P.H. and van den Hondel,C.A. (1987) Transformation of *Aspergillus* based on the hygromycin B resistance marker from *Escherichia coli*. *Gene*, **56**, 117–124.
49. Chu,Z., Li,J., Eshaghi,M., Karuturi,R.K., Lin,K. and Liu,J. (2007) Adaptive expression responses in the Pol-γ null strain of *S. pombe* depleted of mitochondrial genome. *BMC Genomics*, **8**, 323.
50. Ausubel,F.M., Brent,R., Kingston,R.E., Moore,D.D., Seidman,J.G. and Struhl,K. (1993) *Current Protocols in Molecular Biology*. John Wiley & sons, Boston, Mass.
51. Zhang,X., Zhao,Q. and Huang,Y. (2013) Partitioning of the nuclear and mitochondrial tRNA 3′-end processing activities between two different proteins in *Schizosaccharomyces pombe*. *J. Biol. Chem.*, **288**, 27415–27422.
52. Meisinger,C., Pfanner,N. and Truscott,K.N. (2006) Isolation of yeast mitochondria. *Methods Mol. Biol.*, **313**, 33–39.
53. Meisinger,C., Sommer,T. and Pfanner,N. (2000) Purification of *Saccharomcyes cerevisiae* mitochondria devoid of microsomal and cytosolic contaminations. *Anal. Biochem.*, **287**, 339–342.
54. Diekert,K., de Kroon,A.I., Kispal,G. and Lill,R. (2001) Isolation and subfractionation of mitochondria from the yeast *Saccharomyces cerevisiae*. *Methods Cell Biol.*, **65**, 37–51.
55. Lemaire,C. and Dujardin,G. (2008) Preparation of respiratory chain complexes from *Saccharomyces cerevisiae* wild-type and mutant

mitochondria : activity measurement and subunit composition analysis. *Methods Mol. Biol.*, **432**, 65–81.
56. Gouget,K., Verde,F. and Barrientos,A. (2008) In vivo labeling and analysis of mitochondrial translation products in budding and in fission yeasts. *Methods Mol. Biol.*, **457**, 113–124.
57. Gould,K.L., Ren,L., Feoktistova,A.S., Jennings,J.L. and Link,A.J. (2004) Tandem affinity purification and identification of protein complex components. *Methods*, **33**, 239–244.
58. Matsuo,Y., Asakawa,K., Toda,T. and Katayama,S. (2006) A rapid method for protein extraction from fission yeast. *Biosci. Biotechnol. Biochem.*, **70**, 1992–1994.
59. Zhao,Z., Su,W., Yuan,S. and Huang,Y. (2009) Functional conservation of tRNase Z^L among *Saccharomyces cerevisiae*, *Schizosaccharomyces pombe* and humans. *Biochem. J.*, **422**, 483–492.
60. Bonnefoy,N., Kermorgant,M., Groudinsky,O. and Dujardin,G. (2000) The respiratory gene *OXA1* has two fission yeast orthologues which together encode a function essential for cellular viability. *Mol. Microbiol.*, **35**, 1135–1145.
61. Dujeancourt,L., Richter,R., Chrzanowska-Lightowlers,Z.M., Bonnefoy,N. and Herbert,C.J. (2013) Interactions between peptidyl tRNA hydrolase homologs and the ribosomal release factor Mrf1 in *S.pombe* mitochondria. *Mitochondrion*, **13**, 871–880.
62. Takeda,K., Starzynski,C., Mori,A. and Yanagida,M. (2015) The critical glucose concentration for respiration-independent proliferation of fission yeast, *Schizosaccharomyces pombe*. *Mitochondrion*, **22**, 91–95.
63. Zuin,A., Gabrielli,N., Calvo,I.A., Garcia-Santamarina,S., Hoe,K.L., Kim,D.U., Park,H.O., Hayles,J., Ayte,J. and Hidalgo,E. (2008) Mitochondrial dysfunction increases oxidative stress and decreases chronological life span in fission yeast. *PLoS One*, **3**, e2842.
64. Haffter,P. and Fox,T.D. (1992) Nuclear mutations in the petite-negative yeast *Schizosaccharomyces pombe* allow growth of cells lacking mitochondrial DNA. *Genetics*, **131**, 255–260.
65. Wiley,D.J., Catanuto,P., Fontanesi,F., Rios,C., Sanchez,N., Barrientos,A. and Verde,F. (2008) Bot1p is required for mitochondrial translation, respiratory function, and normal cell morphology in the fission yeast *Schizosaccharomyces pombe*. *Eukaryot. Cell*, **7**, 619–629.
66. Kim,D.U., Hayles,J., Kim,D., Wood,V., Park,H.O., Won,M., Yoo,H.S., Duhig,T., Nam,M., Palmer,G. *et al.* (2010) Analysis of a genome-wide set of gene deletions in the fission yeast *Schizosaccharomyces pombe*. *Nat. Biotechnol.*, **28**, 617–623.
67. Matsuyama,A., Arai,R., Yashiroda,Y., Shirai,A., Kamata,A., Sekido,S., Kobayashi,Y., Hashimoto,A., Hamamoto,M., Hiraoka,Y. *et al.* (2006) ORFeome cloning and global analysis of protein localization in the fission yeast *Schizosaccharomyces pombe*. *Nat. Biotechnol.*, **24**, 841–847.
68. Lagouge,M., Mourier,A., Lee,H.J., Spahr,H., Wai,T., Kukat,C., Silva Ramos,E., Motori,E., Busch,J.D., Siira,S. *et al.* (2015) SLIRP regulates the rate of mitochondrial protein synthesis and protects LRPPRC from degradation. *PLoS Genet.*, **11**, e1005423.
69. Suzuki,C.K., Suda,K., Wang,N. and Schatz,G. (1994) Requirement for the yeast gene LON in intramitochondrial proteolysis and maintenance of respiration. *Science*, **264**, 273–276.
70. Van Dyck,L., Pearce,D.A. and Sherman,F. (1994) *PIM1* encodes a mitochondrial ATP-dependent protease that is required for mitochondrial function in the yeast *Saccharomyces cerevisiae*. *J. Biol. Chem.*, **269**, 238–242.
71. van Dyck,L., Neupert,W. and Langer,T. (1998) The ATP-dependent PIM1 protease is required for the expression of intron-containing genes in mitochondria. *Genes Dev.*, **12**, 1515–1524.
72. Su,Y., Yang,Y. and Huang,Y. (2016) Loss of *ppr3*, *ppr4*, *ppr6* or *ppr10* perturbs iron homeostasis and leads to apoptotic cell death in *Schizosaccharomyces pombe*. *FEBS J.*, **284**, 324–337.
73. Hu,J., Wang,K., Huang,W., Liu,G., Gao,Y., Wang,J., Huang,Q., Ji,Y., Qin,X., Wan,L. *et al.* (2012) The rice pentatricopeptide repeat protein RF5 restores fertility in Hong-Lian cytoplasmic male-sterile lines via a complex with the glycine-rich protein GRP162. *Plant Cell*, **24**, 109–122.
74. Huang,W., Yu,C., Hu,J., Wang,L., Dan,Z., Zhou,W., He,C., Zeng,Y., Yao,G., Qi,J. *et al.* (2015) Pentatricopeptide-repeat family protein RF6 functions with hexokinase 6 to rescue rice cytoplasmic male sterility. *Proc. Natl. Acad. Sci. U.S.A.*, **112**, 14984–14989.
75. Bentolila,S., Heller,W.P., Sun,T., Babina,A.M., Friso,G., van Wijk,K.J. and Hanson,M.R. (2012) RIP1, a member of an Arabidopsis protein family, interacts with the protein RARE1 and broadly affects RNA editing. *Proc. Natl. Acad. Sci. U.S.A.*, **109**, E1453–E1461.
76. Takenaka,M., Zehrmann,A., Verbitskiy,D., Kugelmann,M., Hartel,B. and Brennicke,A. (2012) Multiple organellar RNA editing factor (MORF) family proteins are required for RNA editing in mitochondria and plastids of plants. *Proc. Natl. Acad. Sci. U.S.A.*, **109**, 5104–5109.
77. Glass,F., Hartel,B., Zehrmann,A., Verbitskiy,D. and Takenaka,M. (2015) MEF13 requires MORF3 and MORF8 for RNA editing at eight targets in mitochondrial mRNAs in *Arabidopsis thaliana*. *Mol. Plant*, **8**, 1466–1477.
78. Hartel,B., Zehrmann,A., Verbitskiy,D., van der Merwe,J.A., Brennicke,A. and Takenaka,M. (2013) MEF10 is required for RNA editing at *nad2-842* in mitochondria of *Arabidopsis thaliana* and interacts with MORF8. *Plant Mol. Biol.*, **81**, 337–346.
79. Schallenberg-Rudinger,M., Kindgren,P., Zehrmann,A., Small,I. and Knoop,V. (2013) A DYW-protein knockout in *Physcomitrella* affects two closely spaced mitochondrial editing sites and causes a severe developmental phenotype. *Plant J.*, **76**, 420–432.
80. Takenaka,M., Verbitskiy,D., Zehrmann,A., Hartel,B., Bayer-Csaszar,E., Glass,F. and Brennicke,A. (2014) RNA editing in plant mitochondria-connecting RNA target sequences and acting proteins. *Mitochondrion*, **19**, 191–197.
81. Brehme,N., Bayer-Csaszar,E., Glass,F. and Takenaka,M. (2015) The DYW subgroup PPR protein MEF35 targets RNA editing sites in the mitochondrial *rpl16*, *nad4* and *cob* mRNAs in *Arabidopsis thaliana*. *PLoS One*, **10**, e0140680.
82. Baggio,F., Bratic,A., Mourier,A., Kauppila,T.E., Tain,L.S., Kukat,C., Habermann,B., Partridge,L. and Larsson,N.G. (2014) *Drosophila melanogaster* LRPPRC2 is involved in coordination of mitochondrial translation. *Nucleic Acids Res.*, **42**, 13920–13938.
83. Spahr,H., Rozanska,A., Li,X., Atanassov,I., Lightowlers,R.N., Chrzanowska-Lightowlers,Z.M., Rackham,O. and Larsson,N.G. (2016) SLIRP stabilizes LRPPRC via an RRM-PPR protein interface. *Nucleic Acids Res.*, **44**, 6868–6882.